Journal of Integrative Agriculture 2026, 25(3): 1243–1262

Available online at ScienceDirect

Journal of Integrative Agriculture



RESEARCH ARTICLE

Deep storage irrigation can recharge farmland deep soil moisture and sustain production of summer maize (*Zea mays* L.) through flood resources utilization in irrigation districts of northern China

Xiaodong Fan, Xiaotao Hu#, Yakun Wang, Dianyu Chen, Wene Wang, Fang Wang, Qing Zha

Key Laboratory of Agricultural Soil and Water Engineering in Arid and Semiarid Areas of Ministry of Education, Northwest A&F University, Yangling 712100, China

Highlights

- The new technology of "deep storage irrigation" was proposed to utilize flood resources.
- Deep soil moisture recharge occurred when effective rainfall and irrigation exceeded 390 mm.
- Maize grain yield demonstrated a quadratic relationship with deep soil moisture recharge.
- Deep storage irrigation effectively recharged deep soil moisture and maintained maize production.
- Deep storage irrigation showed potential for widespread implementation in irrigation districts of northern China.

Abstract

The irrigation districts of northern China face issues such as water scarcity, inability to effectively utilize flood resources, and groundwater overexploitation. In view of these challenges, this study proposes a new concept of deep storage irrigation through flood resources utilization. However, whether deep storage irrigation can recharge deep soil moisture and sustain crop production still requires further study. A two-year field experiment was conducted on summer maize in the Guanzhong Plain with five soil wetting layer depths (T1: 60 cm; T2: 90 cm; T3: 120 cm; T4: 150 cm; T5: 180 cm) and soil saturation moisture content as the irrigation upper limit. The results presented that the ranges of deep soil moisture recharge in the 100–200 cm soil profile ($SMS_{100–200}$) was 73.34–267.42 and 0–150.03 mm in 2021 (wet season) and 2022 (normal season). When the effective precipitation and irrigation exceeded 390 mm, the $SMS_{100–200}$ began to linearly increase. The highest grain yield (GY) were observed at T2 and T3 treatments in 2021 (11.44 t ha^{-1}) and 2022 (11.25 t ha^{-1}), respectively. The maize GY of T4 in 2021 and T5 in 2022 were only 3.9 and 5.7% lower than the maximize GY, respectively. However, the $SMS_{100–200}$ for T4 and T5 were 2.4 and 5.0 times that of T2 and T3 treatments in 2021 and 2022, respectively. Overall, the further increase in irrigation amounts induced only a slight decrease in grain yield, but it significantly increased deep soil moisture recharge. Therefore, the deep storage irrigation breaks through the traditional idea of water-saving irrigation with limited water resources, which can be utilized as an effective alternative to address the issues of water scarcity, low flood resources utilization, and groundwater level declines in the irrigation districts of northern China.

Keywords: deep storage irrigation, soil moisture dynamics, soil moisture storage, grain yield, summer maize

1. Introduction

The irrigation districts of northern China have long faced the severe challenge of the insufficient precipitation, which has seriously constrained agricultural production, especially the high and stable yield of grain crops (Yang J *et al.* 2023; Liu Z J *et al.* 2024; Wang H *et al.* 2024). To effectively address the issue of climate-induced resources scarcity and ensure national food security, the relevant departments have planned and implemented large-scale construction projects of diversion irrigation districts (Sun *et al.* 2017; Zagaria *et al.* 2021). Nonetheless, the swift expansion of irrigated farmland in northern China poses the significant challenge to regional

Received 22 January 2025; Received in revised form 4 May 2025; Accepted 13 June 2025; Available online 14 July 2025
Xiaodong Fan, Mobile: +86-18832016863, E-mail: fanxiaodong9527@163.com; #Correspondence Xiaotao Hu, Mobile: +86-13892816133, E-mail: huxiaotao11@nwsuaf.edu.cn

© 2026 CAAS. Publishing services by Elsevier B.V. on behalf of KeAi Communications Co. Ltd. This is an open access article under the CC BY-NC-ND license (http://creativecommons.org/licenses/by-nc-nd/4.0/). Peer review under responsibility of Editorial Board of *Journal of Integrative Agriculture*.
doi: 10.1016/j.jia.2025.07.013

water shortages (Yuan *et al.* 2023). Taking the Guanzhong Plain in northern China as an example, to overcome the difficulty that natural rainfall fails to meet the water demands of summer maize, over 70% of irrigation water is usually supplemented by groundwater (Niu *et al.* 2019). Currently, more than 2.5 billion m^3 of groundwater is pumped annually, 50% of which is used for farmland irrigation (Wang H L *et al.* 2018). The excessive exploitation of groundwater resources from shallow and deep aquifers for irrigation has resulted in a persistent decline in water table. This decline has induced severe groundwater depletion and the other environmental problems in aquifers, and thereby threatens the sustainability of groundwater systems, regional food security, and ecological security (Tan *et al.* 2023; Zhang Q S *et al.* 2024).

In the background of global warming, rising temperatures lead to a future increase in the occurrence of extreme weather events on global to regional scales through intensifying the hydrological cycle and changing the large-scale atmospheric circulation (Ayat *et al.* 2022; Kendon *et al.* 2023; Hidalgo *et al.* 2024). One of the most remarkable manifestations of extreme weather is extreme precipitation events (Luo *et al.* 2024). The IPCC Sixth Assessment Report has proposed that the frequency, intensity, duration, and spatial extent of extreme precipitation are projected to further enhance due to the current global climate fluctuations (IPCC 2023). Extreme precipitation will influence terrestrial water cycle, thereby altering surface runoff patterns and increasing flood risk (Davenport *et al.* 2021), where the future flood risks in mainland China will gradually increase by approximately 10–30% (Yin *et al.* 2021). Observations indicate that the increase in precipitation in northern China is primarily driven by extreme precipitation events and intense convective rainfall (Ji and Tian 2024). The region is characterized by a concentrated rainy season and a high contribution to annual precipitation (Yang J *et al.* 2023; Su *et al.* 2024), which may lead to an abundance of flood resources during the flood season. Therefore, both continuous heavy rainfall and flash extreme precipitation may lead to flood disasters, and thus result in the seasonal flooding overflow in the irrigation districts (Wang *et al.* 2022; Fu *et al.* 2023). However, the total reservoir capacity of regulating reservoirs in diversion irrigation districts is generally small, resulting in ineffective utilization of flood resources in the irrigation areas, such as in the Baojixia Irrigation District and Jinghuiqu Irrigation District in the Guanzhong Plain (Gao *et al.* 2021), where exist problems of water scarcity, groundwater overexploitation, and flood resources waste. Therefore, it is imperative to investigate more sustainable irrigation strategy to alleviate the ongoing decline of groundwater table and ensure food production by maximizing utilization of available flood resources in existing farm infrastructure in semi-arid areas with limited water resources.

Overall, a new strategy of deep storage irrigation is proposed in answer to the problems large amounts of water abandonment over the flood seasons and continuous decline in groundwater levels caused by insufficient regulation capacity of reservoir. The concentrated precipitation time in the irrigation districts is forecasted based on a specific probability distribution followed by the long-term hydrological sequence, and reservoir capacity is vacated through flood discharge before the flood seasons. The farmlands in this study are regarded as groundwater recharge surfaces with the saturated moisture content set as the irrigation upper limit. The large-quota and long-duration irrigation is conducted by utilizing water conveyance systems in irrigation districts without significantly decreasing crop yields. On one hand, deep storage irrigation would enable maximizing the excess moisture storage in the deep soil layers, and thus delay the adverse effect of drought conditions progression on maize production and conserve conventional irrigation water consumption. From a functional viewpoint, the soil aquifers serve as natural underground reservoirs that store incoming water from precipitation or irrigation events (Morris *et al.* 2003). Due to the enormous storage capacity of aquifers, they can provide a continuous water source for crops, even during dry seasons when rainfall is almost absent and surface water is quickly exhausted (Camp *et al.* 2010). On the other hand, deep storage irrigation recharges the groundwater resources over dry seasons and regulates the spatial distribution of moisture, which has the potential function to recharge groundwater, and thereby delays the continuous decline of groundwater tables and maintains the normal ecological service of the ecosystem. However, the prolonged duration of large-quota irrigation, especially when combines with precipitation, may increase the risks of flooding or waterlogging damage to crops, and thus lead to crop yield reduction.

The summer maize (*Zea mays* L.) is one of the predominant crops planted in northern China, with the covered area accounting for more than 60% of the cultivated land (Shan *et al.* 2020; Cao *et al.* 2022; Peng *et al.* 2023). The region is preponderant by a semi-humid and semi-arid climate, and unique geographical location and meteorological conditions result in the significant total amount of precipitation resources, while the spatial and temporal distribution of precipitation is highly unstable (Liu Y Z *et al.* 2024; Peng *et al.* 2023). Taking Guanzhong Plain as an example, the annual precipitation has differed widely from 288 to 959 mm over the past 50 years, and 65% of precipitation occurs as storms between July and September (summer maize growing seasons) (Fang *et al.* 2021; Yan S C *et al.* 2022). Although the precipitation capacity seems to basically meet the water demand of summer maize (423 mm reported by Liu *et al.* 2002), the uneven distribution of precipitation over maize growth period results in the maize production constrained by water storage (Zhang *et al.* 2022; Yang B *et al.* 2023). In addition, the mean temperature is high over the maize growing seasons, resulting in a large amount of potential evapotranspiration, and thereby the prominent imbalance between precipitation and evapotranspiration greatly aggravates the soil water deficit in this area (Wang Z P *et al.* 2018; Yuan *et al.* 2018). The frequency of extreme precipitation on consecutive days during the maize grain filling stage follows a significant increasing trend compared to the 46-year mean (1966–2012) in semi-arid areas of northern China, and the occurrence probability of seasonal floods is expected to increase further in the future (Sun *et al.* 2023). Overall, it is reasonable to select summer maize as the

research subject to determine the feasibility of deep storage irrigation in this study.

Notably, the majority of existing research have increasingly used deficit irrigation aimed at water conservation as means to adapt agriculture to water resources shortage, which have primarily concentrated on physiological and agronomic performance of crop plants in response to the water-saving irrigation techniques (Fan *et al.* 2024; Wu *et al.* 2024; Xu *et al.* 2024). Likewise, extensive research has been conducted on the deficit irrigation combined with other measures, such as fertilization strategies, tillage patterns, and biochar amendment, for efficient utilization of water, fertilizer, and heat to achieve sustainable crop production (Zhao *et al.* 2023; Zhang P Y *et al.* 2024). However, there only remains a scarcity of knowledge concerning on the applications of flood resources for agricultural production, and even the few existing studies mostly center on the muddy water irrigation (Guo 2009), which aims to fully utilize sediment particles, dead branches and leaves, and surface mature soil carried by flood to improve soil structure, restore saline-alkali soils and increase soil nutrients, while there are clear regional limitations in practical application. This study proposes to use reservoir water withdrawal or flood resources for deep storage irrigation before flood seasons, which breaks through the traditional patterns of water-saving irrigation with limited water resources in irrigation districts, thereby realizing spatial moisture storage in exchange for extended irrigation time and recharging deep soil moisture. We hypothesize deep storage irrigation can recharge farmland deep soil moisture and sustain crop productivity. To validate this hypothesis, the Guanzhong Plain was taken as the typical study area, and the Baojixia Irrigation District was chosen as the most representative site. Hence, this study aimed to: (1) analyze the feasibility and characteristics of deep soil moisture recharge in farmland under deep storage irrigation; (2) evaluate the influences of deep storage irrigation on maize yield and determine whether it could lead to a significant yield reduction. Deep storage irrigation recommended in this research would provide a sustainable practice in the face of water resources shortage and flood resources waste in semi-arid area, which contributes to the coordinated development of environmental sustainability and food security.

2. Materials and methods

2.1. Experimental site description

The summer maize field experiment was implemented at Caoxinzhuang Experimental Farm located in Baojixia Irrigation District in the Guanzhong Plain, China (34°30′N, 108°09′E; 530 m a.s.l.) (Fig. 1). The Baojixia Irrigation District typically characterizes the northern irrigation districts, thus this irrigation district was selected as a representative district. This region is situated in a semi-humid and drought-prone region, where the average annual temperature, precipitation (1984–2023), and the mean annual pan evaporation are 12.9°C, 558.7 mm, and 1,500 mm, respectively. During the summer maize growing period, the mean temperature and rainfall were 24.1°C and 442.4 mm in 2021, and 24.6°C and 321.9 mm in 2022, respectively (Fig. 2). The experimental site is characterized by a silty clay loam soil texture according to the US Department of Agriculture's Soil Taxonomy, with a field capacity of 25.0% (soil mass moisture content, the same below), a saturated moisture of 31.3%, and soil bulk density of 1.47 g cm^{-3} in the top 200 cm of the soil. The depth of groundwater table in the study area exceeds 60 m, and the vadose zone aquifer has a large thickness with massive accumulation of detrital filling, providing favorable conditions for water storage.

2.2. Experimental design

The maize variety Zhengdan 958 was sown for this experiment because of its universal growth in this area (Lu J S *et al.* 2021). On June18, 2021 and June 20, 2022, summer maize was sown at 70,000 plants ha^{-1} in rows spaced 70 cm and plants spaced 20 cm apart, which was harvested on October 10 in 2021 and September 30 in 2022. This density ensured sufficient space for individual plant development, while preserved field representative conditions for phenotypic measurements. The fertilization rates were 180 kg ha^{-1} nitrogen fertilizer (urea, 46% N; Shaanxi Weihe Heavy Chemical Co., Ltd., China), 80 kg P_2O_5 ha^{-1} diammonium hydrogen phosphate (42% P_2O_5; Shaanxi Baoji Fenghe Chemical Co., Ltd., China), and 60 kg K_2O ha^{-1} potassium sulfate (52% K_2O; Russia Import Trading Company, Russia), which were all spread as basal fertilizers prior to sowing. Maize plants were protected from weeds, nutrient deficits, and insect pests. Five consecutive phenological stages throughout the maize growing season were determined to examine the effects of different irrigation amounts. These stages were planting–V10 (10-leaf), V10–VT (tasseling), VT–R2 (blister), R2–R4 (dough), and R4–R6 (black layer, physiological maturity).

The maize field experiment set up five soil wetting layer depths used for deep storage irrigation, designated as 60, 90, 120, 150, and 180 cm, and 60 cm was regarded as the control treatment (CK). The irrigation amounts were calculated based on the soil moisture content on the day before deep storage irrigation and different soil wetting layer depths, and the irrigation upper limit was set as the soil saturated moisture content. Innovatively, the traditional scientific irrigation methods typically take field capacity as the irrigation upper limit, whereas deep storage irrigation proposed in this study takes the soil saturated moisture content as the irrigation upper limit. The irrigation treatment nomenclatures, irrigation amount calculations, and the calculations of additional irrigation amount compared to the traditional scientific irrigation are detailed in Section 2.3. The five irrigation treatments represented five soil water conditions, and the design scheme along with irrigation amounts are presented in Table 1. The plots were randomly allocated to the five irrigation treatments. In total, 15 plots were divided because each treatment was performed in triplicate. Each plot measured 3 m×6 m, and a 1.2 m buffer zone was set to reduce mutual interferences between adjacent plots. The plot was ridged around the ground, and the plastic baffles with a depth of 2 m relative to the soil surface were buried on all sides of the field bund (Fig. 3).

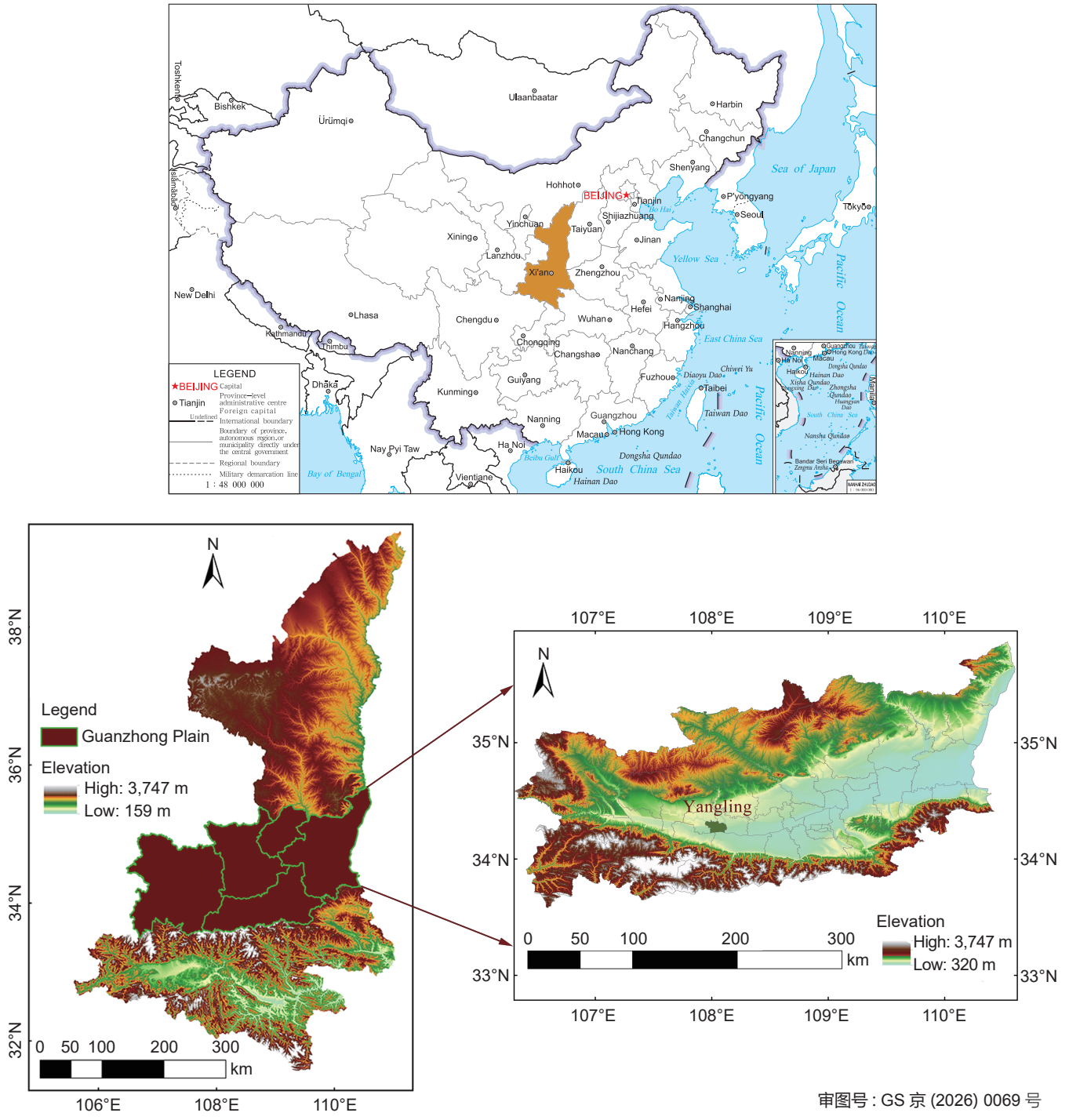


Fig. 1 Geographic location of Yangling in the Guanzhong Plain of Shaanxi Province, China.

Based on the precipitation frequency analysis in the study site over the past decade, surface water was utilized for deep storage irrigation during the jointing stage of summer maize (peak water demand stage, August 4–6) due to more than 50% probability of rainstorms and floods occurring at the jointing stage of maize plants in the Guanzhong Plain. The low-pressure tube water transportation system was fixed for deep storage irrigation, and irrigation water was uniformly poured into each plot. To track the water amount poured into each plot, a flow meter was installed at the hydrant of the system. Supplementary irrigation was applied exclusively between sowing and emergence over the maize growing seasons. The designed moistening layer of the soils was set as 40 cm. Supplementary irrigation started when the soil moisture content in the designed moistening layer reached 60% field capacity, and the irrigation upper limit was equal to 90% field capacity. No supplementary irrigation was applied after maize emergence.

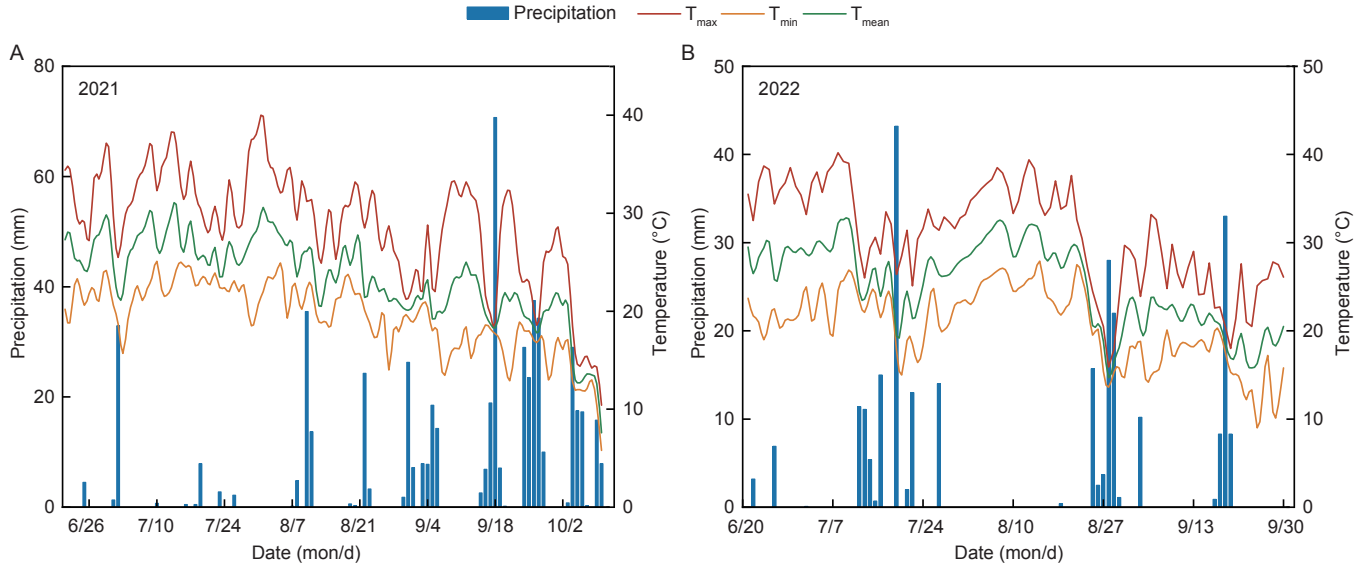


Fig. 2 Daily precipitation, maximum temperature (T_{max}), minimum temperature (T_{min}), and mean temperature (T_{mean}) during the maize growing seasons in 2021 (A) and 2022 (B) in Yangling, China.

Table 1 Irrigation amounts for five irrigation treatments during the maize growing seasons in 2021 and 2022 in Yangling, China

Year	Soil wetting layer depths and abbreviation	Total irrigation amounts (mm)
2021	60 cm (T1)	110.91
	90 cm (T2)	195.42
	120 cm (T3)	250.44
	150 cm (T4)	297.18
	180 cm (T5)	350.22
2022	60 cm (T1)	65.67
	90 cm (T2)	133.32
	120 cm (T3)	176.64
	150 cm (T4)	220.47
	180 cm (T5)	305.61

2.3. Calculation of deep storage irrigation amount

The deep storage irrigation amount (M, mm) is calculated based on the soil moisture content on the day before deep storage irrigation (θ_0, %) and different soil wetting layer depths (H, mm), and the upper limit of irrigation was set as the soil saturated moisture content (θ_{sat}, %). Compared with the traditional irrigation scheduling, the additional irrigation amount of deep storage irrigation (AM, mm) is calculated based on the difference between soil saturated moisture content and soil field capacity (θ_{FC}, %), as well as different soil wetting layer depths (H, mm).

$$M=(\theta_{sat}-\theta_0)\times\gamma_s\times H \quad (1)$$

$$AM=(\theta_{sat}-\theta_{FC})\times\gamma_s\times H \quad (2)$$

where γ_s denotes soil bulk density (g cm^{-3}). As mentioned before, θ_{sat}, θ_{FC}, and γ_s of this experimental farmland are

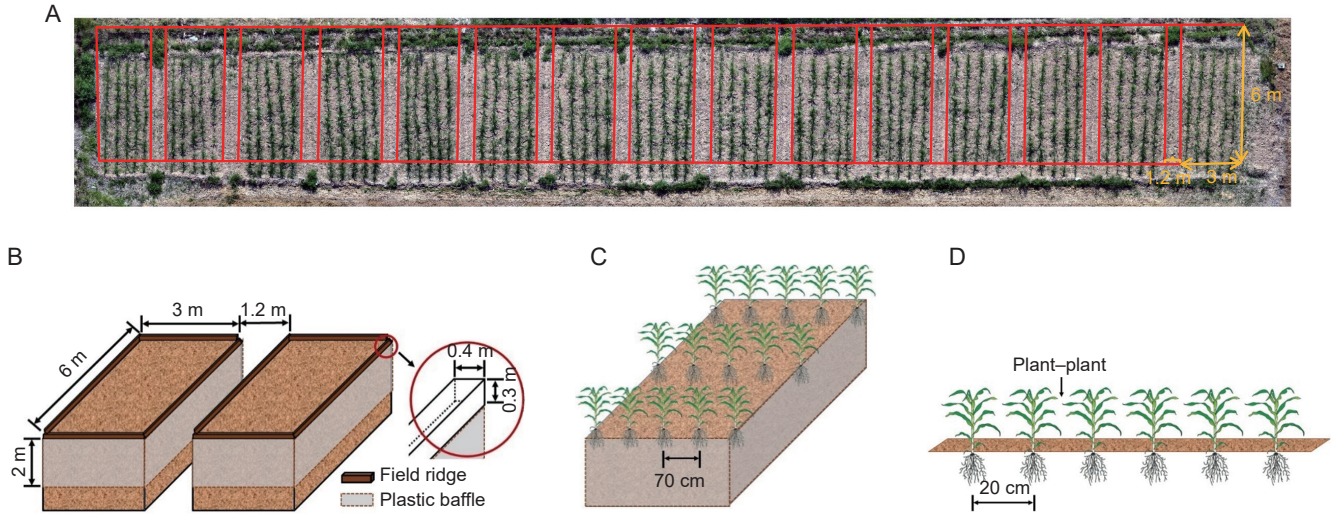


Fig. 3 Schematic diagram of experimental design. A, division map of the test area. B, layout of the deep storage irrigation experimental zone. C, schematic illustration of summer maize planting arrangement in experimental plot. D, diagram of plant spacing in the profile.

31.3%, 25.0%, and 1.47 g cm^{-3}, respectively. This maize field experiment set up five soil wetting layer depths used for deep storage irrigation, which were 60, 90, 120, 150, and 180 cm, respectively. Thus, the AM corresponding to different soil wetting layer depths are 55.57, 83.35, 111.13, 138.92, and 166.70 mm, which were named T1, T2, T3, T4, and T5 treatment, respectively, in the same order.

2.4. Division of precipitation type years

Precipitation during each maize growing season was categorized as wet, normal or dry to analyze soil moisture dynamics and maize yields responses to different irrigation treatments in different precipitation type years.

$$\begin{aligned} &\text{Wet season: } P_i > P+0.33\sigma \\ &\text{Normal season: } P-0.33\sigma \le P_i \le P+0.33\sigma \\ &\text{Dry season: } P_i < P-0.33\sigma \end{aligned} \quad (3)$$

where P_i denotes the precipitation of i maize season (mm), P denotes mean precipitation for the maize seasons from 1984 to 2022 (mm), and σ denotes the standard deviation of P (mm). For summer maize, the average seasonal precipitation from 1984 to 2022 was 337.8±141.2 mm; that is, P_i>384.4 mm for wet season, P_i<291.2 mm for dry season, and 291.2≤P_i≤384.4 mm for normal season. The precipitation in maize seasons were 442.4 and 321.9 mm in 2021 and 2022, respectively. Thus, the maize seasons during the experimental period were wet and normal season, respectively.

2.5. Sampling and measurements

Measurement of soil moisture content Manual sampling and measurements of gravimetric soil moisture content (SMC) were performed for each plot using the oven-drying method (Yan Z J *et al.* 2022). Soil samples were taken from the topsoil (upper 0–2 m) using a hand auger at the center of each plot as the measuring point, with depth of 0–1 m measured in 10 cm increment and depths of 1–2 m measured in 20 cm increment. The samples were then packed into zip-lock bags, sealed immediately to prevent water loss and coded. The soil samples were subsequently transferred to the laboratory on the same day. The soil samples were weighed and dried for 24 h at 105°C, and then weighed again to determine SMC. The SMC was measured on the day before deep storage irrigation to calculate the irrigation amount, then every 10–15 d after the end of treatment according to the weather conditions. Moreover, the additional measurements were carried out after irrigation and heavy rainfall. The SMC of each treatment was measured by averaging SMC of triplicate experiments. After taking soil samples with a hand auger, the boreholes were promptly and meticulously backfilled to ensure the restoration of soil structure to the greatest extent possible. The backfilling process was conducted in layers, with the soil gently compacted to minimize disruption to the soil profiles.

Calculations of soil moisture storage The calculation formulas for the soil moisture storage (SMS, mm) and effective soil moisture storage (SMS_E, mm) are as follows (Yang *et al.* 2021):

$$SMS = SMC \times \gamma_s \times SD \quad (4)$$

$$SMS_E = (SMC - \theta_{PWP}) \times \gamma_s \times SD \quad (5)$$

where γ_s denotes soil bulk density (g cm^{-3}), SD represents soil depth (mm), and θ_{PWP} denotes the permanent wilting point (w/w, %), respectively. θ_{PWP} of our experimental farmland is 6.0 (w/w, %).

Calculations of actual evapotranspiration The actual evapotranspiration (ET_a, mm) was determined by using the water balance approach (James 1988).

$$ET_a = P_e + I + G - (W_t - W_0) - R - D \quad (6)$$

where P_e is the effective precipitation calculated by actual precipitation collected from the automatic weather station close to the study site (mm); I is the irrigation amount (mm); and G represents the groundwater capillary rise (mm), which was negligible as the groundwater table was lower than 60.0 m over the growing period. W_0 and W_t represent SMS in the 0–2 m soil profile at sowing along with maturity (mm), respectively. R is surface runoff (mm), which was considered negligible because it was blocked by the boundary dikes around each plot. D is the amount lost to deep percolation (mm). Notably, D in eq. (6) only refers to the loss by deep percolation resulting from deep storage irrigation. If available water in the root zone (0–1 m) and total applied water by deep storage irrigation were above the field capacity, it would be assumed that the water amount above field capacity leaked into the deeper soil zones and was called deep soil moisture recharge (D: available total water at 0–1 m soil depth before irrigation+applied irrigation water–field capacity) (Kanber *et al.* 1993). Approximately 95% of the maize roots are on the top 60 cm soil depth, less than 2% of root dry weight is in the soil layer below 80 cm, and far fewer roots extended to deeper soil layer below 120 cm (Zhou *et al.* 2008). Therefore, the water absorption by maize root systems largely led to soil water consumption in the 0–100 cm soil layer. In this study, the SMS in the 0–1 m soil layer is considered shallow SMS, whereas that below 1 m and groundwater reserve are considered deep SMS.

Effective precipitation (P_e) is defined as the part of total precipitation, which is available to satisfy crop water requirements (Hershfield 1964). The most detailed definition by FAO describes the P_e as the amount of annual or seasonal precipitation used for crop production in direct and/or indirect ways including the evapotranspiration losses during the growing seasons, evaporated water from the soil surface, water intercepted vegetation cover and certain fractions contributing leaching and percolation losses related with the crop growth (Dastane 1978). Hence, surface runoff, deep percolation losses, and excess moisture in the soil are classified as ineffective (Dastane 1978). Effective precipitation is a parameter of climatic factors, soil cover, site management, topography, etc.

In this study, the fixed percentage of precipitation (FP) is used to calculate the effective precipitation. FP is the most primitive version of effective precipitation calculation methods. In this method, the P_e is modeled as a certain fraction of the average precipitation (eq. (7)). This fraction (α) is usually specified to be between 70 and 100% of total precipitation in which the surface runoff and deep percolation losses are assumed to be around 0–30% (Smith *et al.* 1992; Pongpinyopap and Mungcharoen 2012). The method has been applied for α values of 0.7–0.8, 0.8–1.0, and 1.0, and the formula is as follows:

$$P_e=\alpha\times P \quad (7)$$

where P denotes the precipitation amount (mm), and α represents the effective utilization coefficient. When P≥50 mm, α is 0.7–0.8; 5 mm<P≤50 mm, α is 0.8–1.0; P≤5 mm, α is 1.0 (Kang and Cai 1996).

Calculations of average soil moisture content in different soil layers The soil profile was divided into two layers (0–100 and 100–200 cm) to analyze the average soil moisture content (ASMC) in the shallow and deep soil layers under different irrigation treatments. The fluctuation range of ASMC for different irrigation treatments within the same soil layer (0–100, 100–200, and 0–200 cm) was defined as the range between the minimum and maximum values of ASMC calculated for those irrigation treatments in that soil layer. The calculation formula for ASMC (%) in the 0–100, 100–200, or 0–200 cm soil profile is as follows:

$$ASMC=SMS/\gamma_s/10 \quad (8)$$

where SMS denotes the soil moisture storage in the 0–100, 100–200, or 0–200 cm soil profile (mm), and γ_s denotes soil bulk density (g cm^{-3}).

Measurement of grain yield and yield components At the physiological maturity of summer maize (over 75% of maize kernels had black layers), 20 maize plants growing uniformly were manually harvested in an area of 0.7 m-width and 6.0 m-length (the two unsampled rows in the middle) from each plot, and the grains were manually separated from the cobs. The grain yield (GY) was measured when the grains were air dried and reached the standard moisture content of 14% (Mansouri-Far *et al.* 2010). In addition to the two border rows in each plot, the harvested samples were obtained in each sampled row at least 1 m from the field ridges to prevent edge effects. Ten randomly chosen maize ears were selected for the measurements of phenotypic features from each plot in the central row, and the average was recorded. Specifically, a vernier caliper was used to measure the bald tip length (BL), grain length (GL), grain width (GW), ear diameter (ED), corncob diameter (CD). A ruler was utilized to measure the ear length (EL), and an electronic scale with an accuracy of 0.01 g was used to measure the 100-kernel weight (HKW).

2.6. Statistical analysis

Statistical analyses were conducted using one-way analysis of variance to investigate the effects of deep storage irrigation on soil moisture content of different irrigation treatments and soil layers, actual evapotranspiration, soil moisture storage variations in the shallow and deep soil profiles, grain yield and yield components of summer maize using the General Linear Model Full Factorial Mode, followed by Duncan's multiple range test (P<0.05) by using SPSS v. 26.0 software (IBM, Chicago, IL, USA). The least significant difference test was utilized to identify significant variations between treatment groups (Razaq *et al.* 2017). Adobe Illustrator 2020 (Adobe Systems., San Jose, CA, USA) and Origin 2023 (OriginLab Inc., USA) were employed for the creation of the figures.

3. Results

3.1. Average soil moisture content in different soil layers

The soil profile was divided into two layers (0–100 and 100–200 cm) to analyze the ASMC of summer maize in the shallow and deep soil layers under different irrigation amounts (Figs. 4 and 5). The fluctuations of the ASMC were observed in the 0–100, 100–200, and 0–200 cm soil profiles as summer maize development stages progressed during the two growing seasons. The ASMC in the 0–100 cm soil profile ($ASMC_{0–100}$) significantly increased with increasing irrigation amounts after deep storage irrigation in 2021 (P<0.05), and the fluctuation range of $ASMC_{0–100}$ was 21–22% at the end of the growth period (P>0.05; Fig. 4-A–C). Notably, once the irrigation amounts reached a certain extent, $ASMC_{0–100}$ no longer increased sharply as irrigation application amounts increased (Fig. 4), as seen in 2021 as an example. After 10 d of irrigation applications, $ASMC_{0–100}$ changed to 16.34, 19.12, and 20.50% for T1, T2, and T3 treatments, respectively, and thus improved by 17.0 and 25.5% for T2 and T3 treatments, respectively, in comparison to that under T1 treatment (P<0.05). Meanwhile, $ASMC_{0–100}$ was 20.67 and 20.99% for T4 and T5 treatments, respectively, which were 26.5 and 28.5% higher than that under T1 treatment (P<0.05; Fig. 4-A–C). The ASMC in the 100–200 and 0–200 cm soil profiles ($ASMC_{100–200}$ and $ASMC_{0–200}$) gradually increased as irrigation amounts increased, and the soil maintained this variation trend over time in the later growth stages (Fig. 4). Overall, both $ASMC_{100–200}$ and $ASMC_{0–200}$ for each treatment were in the order of T5>T4>T3>T2>T1 at the end of the maize growing period. It can be observed that $ASMC_{0–100}$, $ASMC_{100–200}$ and $ASMC_{0–200}$ reached the highest values in the late growth period, mainly due to the continuous rainfall as the growing seasons progressed in 2021 (Fig. 5-A–E). In contrast, the precipitation frequency and amount decreased in 2022, and ASMC in the different soil layers reached peak values after deep storage irrigation (Fig. 5-F–J).

3.2. Soil moisture storage variations in the shallow and deep soil layers

Dynamic changes in SMS in the different soil layers differed with deep storage irrigation amounts and maize growth stages (Table 2). The water consumption of summer maize was reflected in the variations of SMS. During the planting–V10 stage, the soil water supplement was less than the soil water consumption in the 0–100 cm soil layer under different irrigation amounts, and thus the variations of SMS in the 0–100 cm soil profile ($SMS_{0–100}$) was negative during this stage. In contrast, the variations of $SMS_{0–100}$ was positive in 2022, mainly due to the significant increase in water supplement compared to water consumption over the planting–V10 (Fig. 6). Notably, deep storage irrigation was not applied on summer maize over planting–V10, and the soil water supplement was solely provided by rainfall. Therefore, there was no difference in the variations of $SMS_{0–100}$ between different irrigation treatments (P>0.05). During the V10–VT, the increments of $SMS_{0–100}$ showed significant differences under different irrigation treatments due to different irrigation amounts for plants (P<0.05). The increments of $SMS_{0–100}$ gradually increased with an increase in irrigation amounts for all irrigation treatments and reached the highest values under T5 treatment. The difference is that the variations of

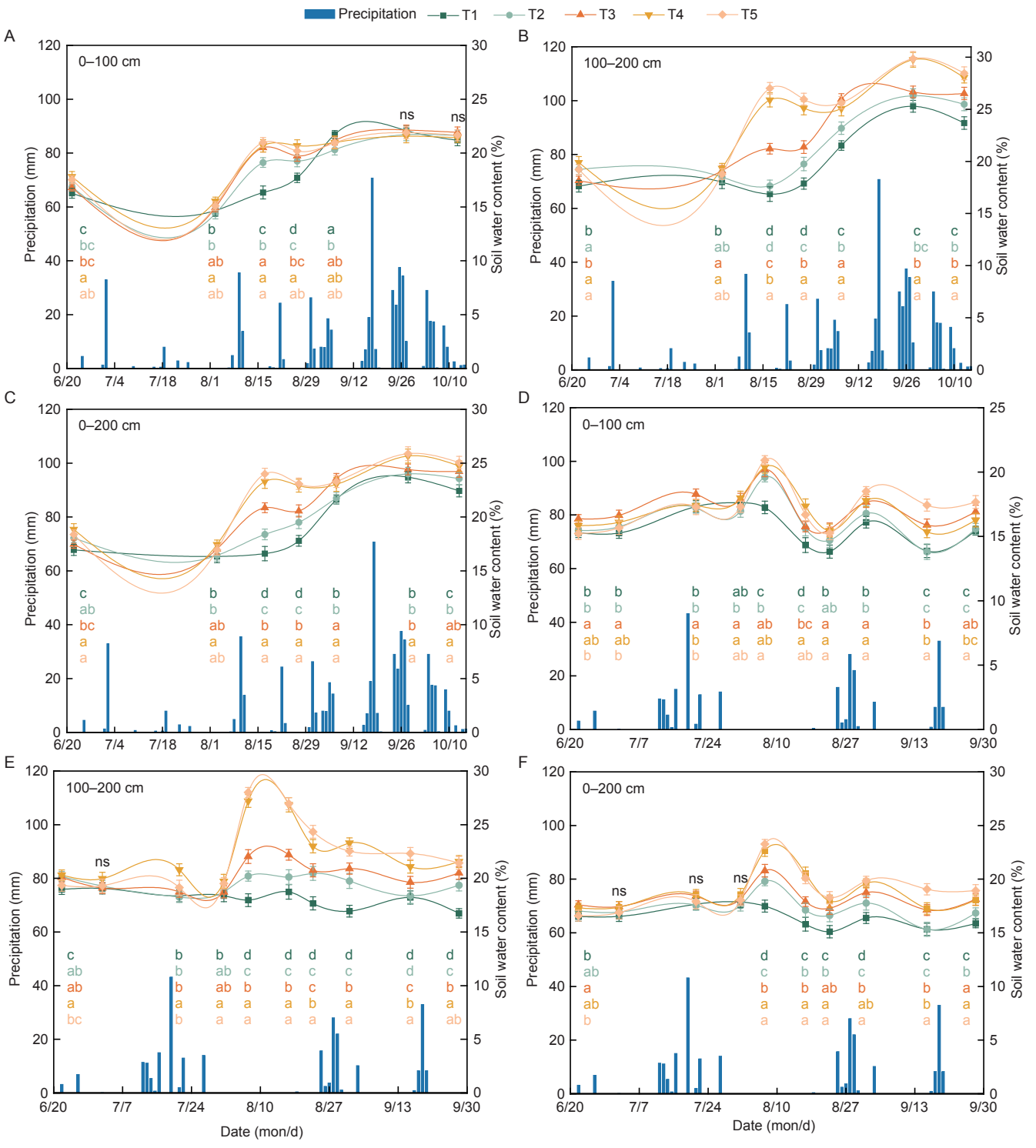


Fig. 4 Average soil moisture contents in the 0–100, 100–200 and 0–200 cm soil profiles under different irrigation treatments during the summer maize growing seasons in 2021 (A–C) and 2022 (D–F) in Yangling, China. Error bars indicate the standard deviation of the mean values (n=3). The different lowercase letters denote significant differences between different irrigation treatments in the same soil layers at the P<0.05 significance level. ns indicates no significant differences at the P<0.05 significance level. T1, T2, T3, T4, and T5 treatments correspond to five soil wetting layer depths of 60, 90, 120, 150, and 180 cm utilized for deep storage irrigation, respectively.

$SMS_{0–100}$ for different irrigation treatments was positive in 2021 and negative in 2022, mainly due to the larger irrigation amounts (Table 1) and supplementary rainfall (Fig. 6) in 2021. Moreover, the deep soil moisture recharge in the 100–200 cm soil profile ($SMS_{100–200}$) was produced under different irrigation treatments during the V10–VT stage, and significantly increased with irrigation amounts increasing (P<0.05). The peak $SMS_{100–200}$ was achieved under T5 treatment in 2021 (207.94 mm) and 2022 (150.03 mm). During the VT–R6, the fluctuations of $SMS_{0–100}$ in different irrigation treatments were

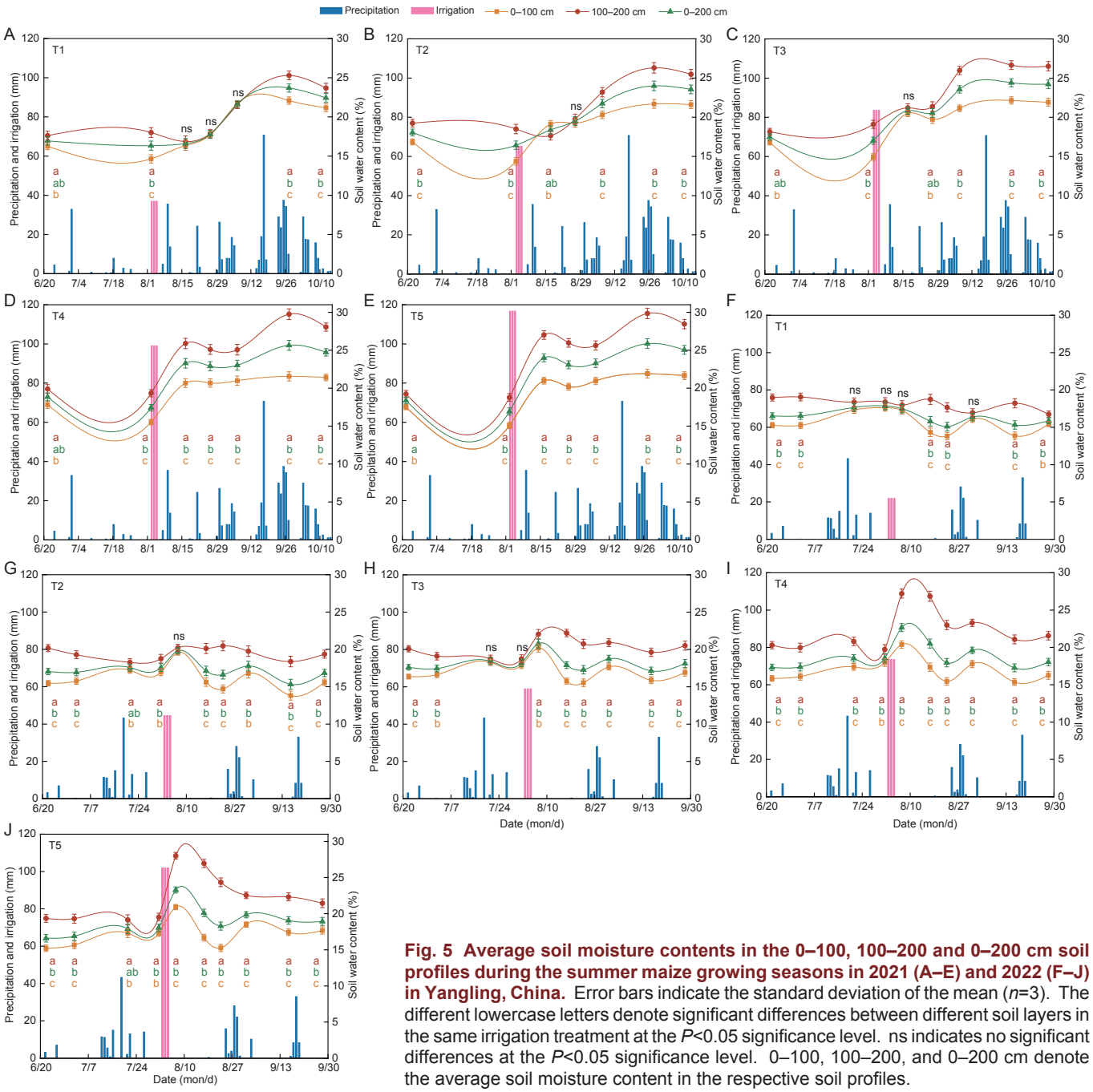


Fig. 5 Average soil moisture contents in the 0–100, 100–200 and 0–200 cm soil profiles during the summer maize growing seasons in 2021 (A–E) and 2022 (F–J) in Yangling, China. Error bars indicate the standard deviation of the mean (n=3). The different lowercase letters denote significant differences between different soil layers in the same irrigation treatment at the P<0.05 significance level. ns indicates no significant differences at the P<0.05 significance level. 0–100, 100–200, and 0–200 cm denote the average soil moisture content in the respective soil profiles.

induced through rainfall and evapotranspiration. Moreover, the deep soil moisture recharge was induced by the heavy rainfall over R4–R6 in 2021, but there was no difference in the variations of $SMS_{0–100}$ among the different irrigation treatments (Table 2; Fig. 6).

The proportions of variations of SMS to the effective rainfall and irrigation amounts differed in the 0–100 and 100–200 cm soil layers among different irrigation treatments during the summer maize growing seasons (Table 3). The variations of $SMS_{0–100}$ fluctuated from 58.35 to 88.18 mm, which accounted for 8.86–20.13% of the sum of effective precipitation and irrigation for different irrigation treatments in 2021, and the values were 2.90–35.37 mm and 0.79–6.57% in 2022. The amounts and proportions of deep soil moisture recharge significantly increased with increasing irrigation amounts (P<0.05). The respective spans of $SMS_{100–200}$ were 73.34–267.42 mm in 2021 and 0–150.03 mm in 2022, and the respective proportions were 16.74–37.59 and 0–27.86% in 2021 and 2022.

3.3. Summer maize yields characteristics

The maize GY and yield components of different irrigation treatments in 2021 and 2022 growing seasons are shown in Table 4. Deep storage irrigation significantly affected maize GY (P<0.05), whereas only had limited effects on yield components in 2021 (P>0.05). The GY increased with an increase in the irrigation amounts, until reaching the maximum GY at T2 treatment (11.44 t ha^{-1}) and then slowly decreased. The averaged GY were 11.32 and 10.99 t ha^{-1} for T3 and T4 treatments, respectively, which were only 1.05

Table 2 The variations of soil moisture storage (SMS) in the 0–100 and 100–200 cm soil profiles under different irrigation treatments during different maize growing stages in 2021 and 2022 in Yangling, China

Soil layer treatments[1)]	Shallow soil moisture storage variations in 0–100 cm (mm)[2)]				Deep soil moisture storage increments in 100–200 cm (mm)				
	Planting–V10	V10–VT	VT–R2	R2–R4	R4–R6	Planting–V10	V10–VT	VT–R2	R2–R4	R4–R6
2021										
T1	–25.89±9.69 a	46.03±10.19 b	–0.18±5.77 a	63.76±14.93 a	4.46±18.28 a	0	0±0 e	0	0	73.34±13.33 a
T2	–39.75±5.84 a	76.48±8.28 a	1.08±2.11 a	16.73±9.17 b	21.45±7.25 a	0	41.78±9.03 d	0	0	50.06±5.69 b
T3	–29.66±11.72 a	88.74±9.97 a	–12.31±0.60 b	21.54±10.93 b	15.57±4.57 a	0	105.66±6.50 c	0	0	62.61±3.06 ab
T4	–36.68±3.19 a	80.93±8.18 a	0.16±3.72 a	5.47±9.43 b	8.47±2.09 a	0	161.92±4.37 b	0	0	60.70±4.25 ab
T5	–39.18±6.68 a	91.54±8.00 a	–11.09±5.33 b	11.91±3.79 b	15.14±3.35 a	0	207.94±4.07 a	0	0	59.48±3.23 b
2022										
T1	37.83±1.42 a	–53.28±8.92 c	28.89±9.43 a	–35.58±8.93 bc	25.06±3.52 a	0	0±0 d	0	0	0
T2	25.27±6.54 a	–22.69±6.48 a	19.05±8.56 ab	–45.88±9.12 c	27.15±0.62 a	0	0±0 d	0	0	0
T3	25.14±6.85 a	–35.62±8.90 b	31.70±8.56 a	–28.11±3.82 ab	16.10±2.41 b	0	30.59±5.99 c	0	0	0
T4	34.41±11.11 a	–13.30±5.52 a	7.53±13.90 b	–37.10±7.86 bc	13.77±5.69 b	0	77.36±10.09 b	0	0	0
T5	29.58±6.09 a	–11.56±2.01 a	29.67±3.94 a	–16.16±2.51 a	3.84±3.84 c	0	150.03±1.46 a	0	0	0

[1)] T1, T2, T3, T4, and T5 treatments denote five soil wetting layer depths of 60, 90, 120, 150, and 180 cm utilized for deep storage irrigation, respectively.
[2)] V10, 10-leaf stage; VT, tasseling; R2, blister; R4, dough; R6, physiological maturity.
Values represent mean±SD (n=3). The different lowercase letters indicate significant differences among different irrigation treatments at the P<0.05 significance level.

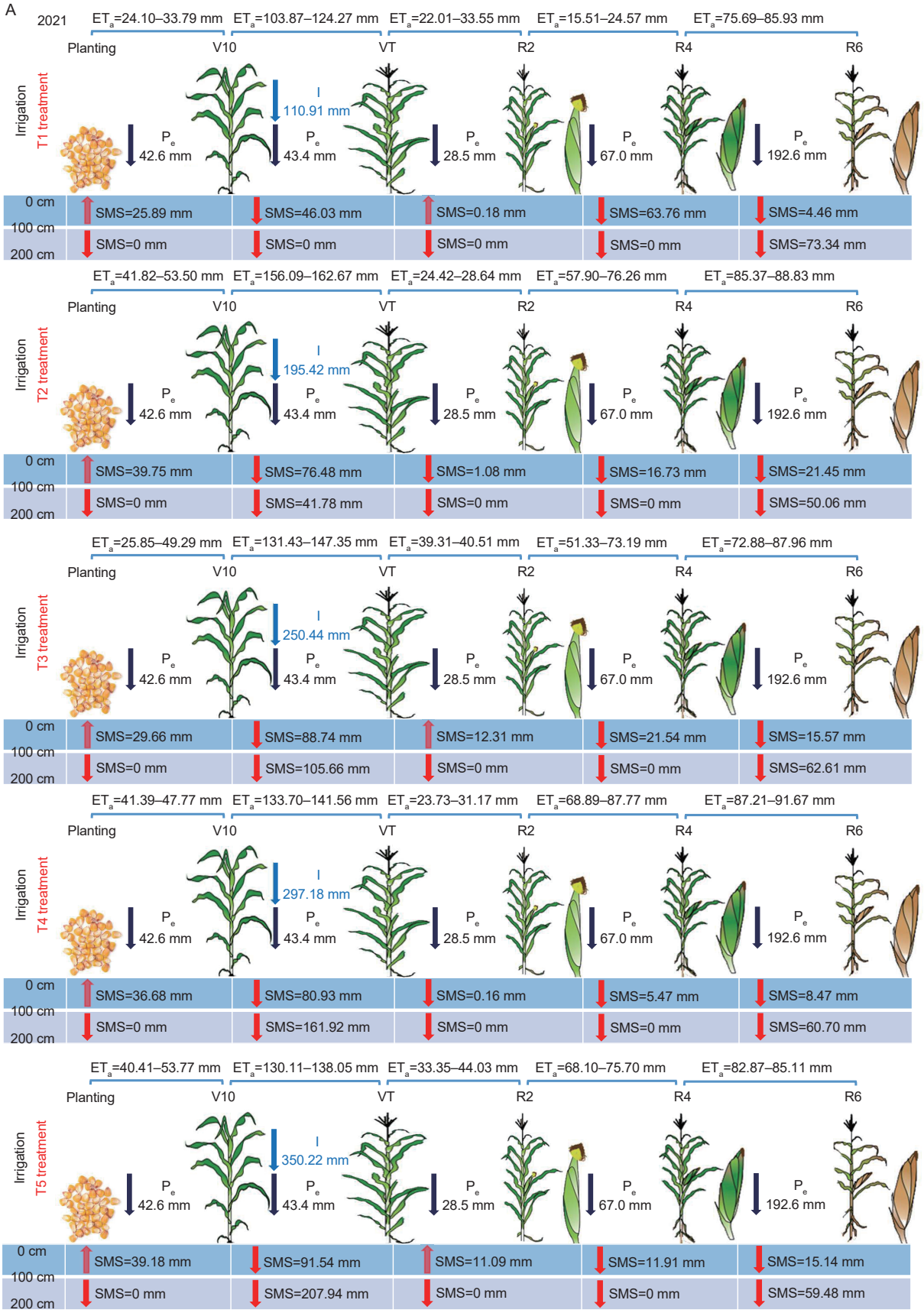
and 3.93% lower than the highest GY produced by T2 treatment, respectively (P>0.05). However, the GY was significantly decreased by 13.81% under T5 treatment compared with that under T2 treatment (P<0.05). Also, the ear rows (ER), GL, ED, CD, and EL of the T5 treatment were less than those under the other irrigation treatments. However, there was no significant difference in the yield components among the different irrigation treatments (P>0.05), which collectively resulted in a smaller GY for T5 treatment in relative to the other treatments. As for the GY in 2022, there was no significant difference among the different irrigation treatments (P>0.05), but the GY of T1 treatment was lower (by 9.68, 11.29, 11.21, and 5.94%, respectively) than the other treatments. The GY first increased and subsequently declined with the irrigation amounts increasing, which achieved a peak value in T3 treatment (11.25 t ha^{-1}). Notably, the T4 and T5 treatments achieved near maximum GY, which was 0.1 and 5.7% lower than the highest GY generated by T3 treatment (P>0.05). The ER, CD, and HKW of T4 treatment were higher than those of the other irrigation treatments, and the BL was smaller than those for the other irrigation treatments, which collectively resulted in the greater GY of T4 treatment compared with T1, T2, and T5 treatments.

3.4. Relationship between deep soil moisture recharge and effective precipitation and irrigation

The Fig. 7 presented the relationship between deep soil moisture recharge and the sum of effective precipitation and irrigation during the whole growth period of summer maize. When the effective precipitation and irrigation did not exceed 390 mm, the deep soil moisture recharge in the 100–200 cm soil layer ($SMS_{100–200}$) did not produce. This phenomenon indicated that soil moisture was mainly distributed in the shallow soil layer of 0–100 cm under the low total water input, and failed to effectively penetrate into the deep soil layer of 100–200 cm, and thereby $SMS_{100–200}$ was not produced. When the effective precipitation and irrigation exceeded 390 mm, the $SMS_{100–200}$ initiated a linear increase, which suggested that soil moisture gradually infiltrated from shallow layers to deep layers, thus beginning to produce $SMS_{100–200}$. For example, when the effective precipitation and irrigation amount reached 430 mm in 2021, the $SMS_{100–200}$ was about 30 mm. Moreover, when the effective precipitation and irrigation was about 470 mm, the $SMS_{100–200}$ reached around 75 mm in both 2021 and 2022. This result further indicated that the $SMS_{100–200}$ exhibited a continuous upward trend with the sum of effective precipitation and irrigation continued to increase.

3.5. Relationships between grain yield and irrigation amounts as well as deep soil moisture recharge

The relationships between GY and irrigation amount as well as deep soil moisture recharge were analyzed (Fig. 8). The significant quadratic function relationships were observed between GY and irrigation amounts during maize growing seasons (Fig. 8-A and B). The GY first improved almost linearly as the irrigation amounts increased until T2 and T3 treatments in 2021 and 2022, respectively, after which GY exhibited a downward trend. Due to the limited grain filling period for summer maize in the Guanzhong Plain, the sufficient water supply postponed anthesis stage, thus shortening the grain filling duration, ultimately resulting in



(Continued on next page)

Fig. 6 Schematic representation of effective precipitation (P_e), irrigation amounts (I), total actual evapotranspiration (ET_a), and the variations of soil moisture storage (SMS) at different soil layers during different maize growth stages under different irrigation treatments from 2021 (A) to 2022 (B) in Yangling, China. V10, 10-leaf stage; VT, tasseling; R2, blister; R4, dough; R6, physiological maturity. ET_a, actual crop evapotranspiration; P_e, effective precipitation; I, irrigation amounts; SMS, soil moisture storage.

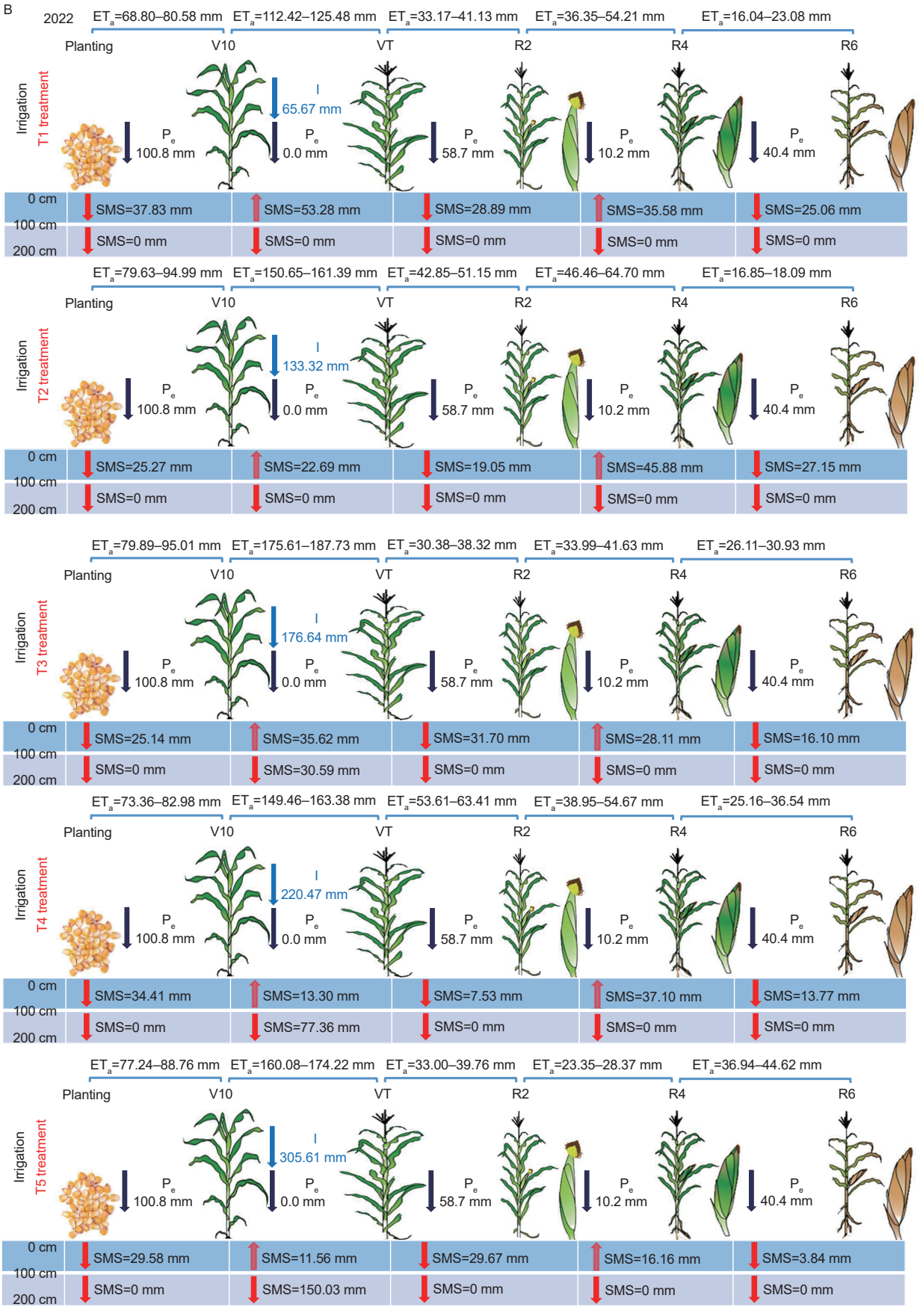


Fig. 6 (Continued from preceding page)

Table 3 Shallow soil moisture storage variations in 0–100 cm, deep soil moisture storage increments in 100–200 cm and total actual growing season evapotranspiration (ET_a) as well as the proportions to total water supply during the summer maize growing seasons in 2021 and 2022 in Yangling, China

Soil layer treatment[1)]	Shallow soil moisture storage variations in 0–100 cm (mm)	Proportion of shallow soil moisture storage variation to total water supply (%)	Deep soil moisture storage increments in 100–200 cm (mm)	Proportion of deep soil moisture storage increments to total water supply (%)	Maize field actual evapotranspiration (mm)	Proportion of maize field actual evapotranspiration of farmland to total water supply (%)
2021						
T1	88.18±4.68 a	20.13±0.77 a	73.34±3.33 e	16.74±0.74 d	276.49±5.21 d	63.12±2.54 b
T2	75.99±3.52 b	13.69±0.54 b	91.84±4.80 d	16.54±0.69 d	387.75±4.02 a	69.77±3.22 a
T3	83.88±4.52 a	13.71±0.59 b	168.27±8.30 c	27.51±0.85 c	359.55±4.12 c	58.78±2.04 c
T4	58.35±2.02 d	8.86±0.35 c	222.62±8.55 b	33.81±1.15 b	377.43±3.54 b	57.32±1.56 c
T5	68.32±3.19 c	9.60±0.41 c	267.42±8.65 a	37.59±1.19 a	375.75±3.78 b	52.81±1.44 d
2022						
T1	2.92±2.85 b	0.98±0.96 b	0±0 d	0±0 d	295.63±2.85 c	99.02±0.96 a
T2	2.90±1.56 b	0.79±0.42 b	0±0 d	0±0 d	363.38±1.56 ab	99.21±0.43 a
T3	9.21±4.16 b	2.25±1.02 b	30.59±5.99 c	7.47±1.46 c	369.80±6.99 a	90.28±1.71 b
T4	5.31±3.81 b	1.17±0.84 b	77.36±10.09 b	17.06±2.23 b	370.76±7.63 a	81.77±1.68 c
T5	35.37±2.11 a	6.57±0.39 a	150.03±1.46 a	27.86±0.27 a	353.17±2.35 b	65.58±0.44 d

[1)] T1, T2, T3, T4, and T5 treatments denote five soil wetting layer depths of 60, 90, 120, 150, and 180 cm utilized for deep storage irrigation, respectively.
Values represent mean±SD (n=3). The different lowercase letters indicate significant differences among different irrigation treatments at the P<0.05 significance level.

a decreased HKW. Likewise, the response of maize GY to deep soil moisture recharge also followed a quadratic curve (Fig. 8-C and D). Specifically, GY first increased and then decreased as deep soil moisture recharge increased. Notably, the T3 and T4 treatments achieved near the highest GY produced by T2 treatment in 2021. However, $SMS_{100–200}$ of T3 and T4 treatments were 1.8 and 2.4 times that of T2 treatment, respectively. The GY for T4 and T5 treatments were only 0.1 and 5.7% lower compared to the highest GY produced by T3 treatment in 2022, respectively, while the $SMS_{100–200}$ was about 2.5 and 5.0 times that of T3 treatment, respectively. This suggested that deep storage irrigation achieved deep soil moisture recharge and sustained crop production.

4. Discussion

4.1. Spatial patterns analysis of the soil moisture for summer maize

The distribution characteristics of ASMC in the soil profile depend on the water balance among the irrigation amounts, water consumption, and precipitation. Due to the different irrigation and precipitation amounts over maize growing season, the water distribution in the soil layers differed in our experiment (Figs. 4 and 5). To maximize the utilization of available soil water, it is vital to determine reasonable irrigation schemes to achieve appropriate water distribution in the soil profile (Yost *et al.* 2019; Zhao *et al*. 2024). As previously discovered by Allen *et al.* (1998), the soil moisture storage capacity in the root zone of plants refers to the maximum amount of soil moisture that can be stored in the soil profile to support optimal crop growth and yield. It is calculated as the thickness of the root zone multiplied by the difference between the SMC at the field capacity and the permanent wilting point. In this study, the lower deep storage irrigation amounts coupled with rainfall mainly concentrated in the 0–100 cm shallow soil layer. Therefore, the $ASMC_{0–100}$ for the different irrigation treatments significantly increased with an increase in irrigation amounts. Notably, the $ASMC_{0–100}$ no longer sharply increased with increasing irrigation amounts when the irrigation amounts reached a certain extent. It can be inferred that the wetting front advanced downward from the topsoil as irrigation amounts increased, and the thickness of saturated soil layers increased continuously in the 0–100 cm soil layer. The soil moisture recharge exceeding the field capacity migrated to the deeper soil layers due to the gravity and matrix suction, which in turn resulted in an increase in ASMC in the deep soil layers. Hence, $ASMC_{100–200}$ and $ASMC_{0–200}$ gradually increased with increasing irrigation amounts. Because it is not influenced by climate change, agricultural management, or insufficient water absorption by root systems, the spatial patterns of the ASMC in the 100–200 cm soil layer may persist over time. In addition, the fluctuation ranges of the variations of $SMS_{0–100}$ and the proportions to the sum of effective precipitation and irrigation showed significant variations between 2021 and 2022. The larger variations of $SMS_{0–100}$ in 2021 (58.35–88.18 mm) constituted 8.86–20.13% of the sum of effective precipitation and irrigation, whereas the smaller variations in 2022 (2.90–35.37 mm) represented 0.79–6.57% of the sum of effective precipitation and irrigation, which indicates the increments of $SMS_{0–100}$ and its proportions exhibited greater values in 2021 compared to 2022. This phenomenon could be owing to the following two possible reasons. Firstly, the total precipitation and its distribution over the maize growing seasons experienced notable differences between 2021 and 2022, which significantly impacted shallow soil moisture dynamics. As mentioned before, the maize seasons during the experimental period were wet and normal seasons,

Table 4 Summer maize yield and yield components in 2021 and 2022 growing seasons in Yangling, China

Soil layer treatments[1)]	Columns no. per ear	Rows no. per ear	Bald tip length (mm)	Grain length (mm)	Grain width (mm)	Ear diameter (mm)	Corncob diameter (mm)	Ear length (cm)	100-kernel weight (g)	Grain yield (t ha^{-1})
2021										
T1	14.35±0.43 a	37.18±0.83 a	10.18±0.56 a	11.83±0.31 a	10.18±0.56 a	47.98±0.61 a	16.49±0.25 a	16.49±0.24 a	27.89±1.35 a	10.71±0.31 abc
T2	14.10±0.26 a	37.2±1.47 a	9.90±0.72 a	11.99±0.11 a	9.9±0.72 a	48.25±0.55 a	17.00±0.09 a	16.99±0.08 a	29.55±0.63 a	11.44±0.37 a
T3	14.77±0.26 a	37.48±1.25 a	9.96±1.26 a	11.79±0.05 a	9.96±1.26 a	45.89±2.61 a	17.09±0.67 a	17.08±0.67 a	29.08±0.24 a	11.32±0.47 ab
T4	14.00±0.17 a	38.1±1.66 a	8.00±0.75 a	12.19±0.31 a	8.00±0.75 a	48.13±0.82 a	16.84±0.63 a	16.83±0.62 a	29.46±0.33 a	10.99±0.33 ab
T5	14.00±0.29 a	36.75±1.11 a	8.68±0.99 a	11.74±0.17 a	8.68±0.99 a	47.00±0.64 a	15.99±0.3 ab	15.98±0.29 a	28.60±0.48 a	9.86±0.18 bc
2022										
T1	14.67±0.85 a	34.84±0.75 bc	15.25±4.12 a	12.26±0.27 a	9.95±0.26 a	49.00±0.63 c	27.02±1.89 b	18.67±0.30 ab	26.05±1.01 ab	9.98±0.49 ab
T2	16.00±0.20 a	37.67±1.41 ab	12.27±1.9 ab	11.87±0.52 a	10.00±0.37 a	53.18±0.72 a	31.33±0.24 a	19.67±0.61 a	24.92±0.97 ab	11.05±0.46 a
T3	14.67±0.43 a	36.84±1.17 ab	10.72±1.68 ab	12.6±0.33 a	10.16±0.12 a	51.73±0.5 ab	30.12±0.33 a	19.39±0.55 ab	26.74±0.65 a	11.25±0.27 a
T4	15.00±0.45 a	39.34±1.09 a	5.46±1.08 b	12.48±0.32 a	9.91±0.29 a	51.71±0.92 ab	32.16±1.18 a	19.20±0.55 ab	27.05±0.77 a	11.24±0.35 a
T5	15.34±0.43 a	38.67±1.31 a	11.92±1.63 ab	11.36±0.65 a	9.85±0.18 a	51.38±1.15 ab	30.55±0.76 a	18.85±0.46 ab	23.44±1.14 b	10.61±0.58 a

[1)] T1, T2, T3, T4, and T5 treatments denote five soil wetting layer depths of 60, 90, 120, 150, and 180 cm utilized for deep storage irrigation, respectively.
Values represent mean±SD (n=3). The different lowercase letters indicate significant differences among different irrigation treatments at the P<0.05 significance level.

respectively. As a result, the higher and more frequent rainfall events in 2021 caused greater water infiltration and even greater increases in shallow soil moisture storage. Secondly, the actual evapotranspiration of maize field under the same irrigation treatment showed little variation between 2021 and 2022 (Table 3). Therefore, the higher and more frequent rainfall events in 2021 resulted in more water remaining in the shallow soil layer of 0–100 cm, which led to the greater increments of shallow soil moisture storage in 2021.

Generally, the rainfall effect was considered as the main reason for the differences of SMC spatial distribution in the shallow soil layer as shallow soils were more sensitive to rainfall events (Gao *et al.* 2024). Similarly, irrigation probably was the main factor leading to the difference between the shallow and deeper layers in this study, especially with such large amount of water for one event. Most previous studies on spatial-temporal distribution of SMC have been conducted for shallow soils. Limited studies on deeper soils have exhibited that the spatial distribution of soil moisture generally stabilizes with increasing soil depth, largely because shallow soils have highly variable inherent properties, and are susceptible to external impacts such as meteorological conditions, soil biology, compaction, and other physical disturbances (Choi and Jacobs 2007; Korres *et al.* 2015). Other studies reported opposite results that shallow soils had larger stability than the deeper soils (Gao and Shao 2012). Famiglietti *et al.* (2008) reasoned that different controlling factors for soil moisture dynamics determined the SMC spatial distribution. In their case, spatial variability of soil texture was the dominant factor. In the current study, it was expected that spatial variability in soil properties, particularly soil texture, would control SMC spatial distribution. Gao *et al.* (2024) reported that the SMC spatial variability would depend largely upon soil texture. While for shallow soils in agricultural field, heterogeneity in root distribution (root water uptake) likely increased the overall magnitude of SMC spatial variability. Therefore, the spatial variability along the vertical profile might impact SMC spatial distribution randomly. Unfortunately, the extent to which the SMC spatial variability could not be quantified, as SMC spatial variability was not measured in this study.

4.2. Analysis of deep soil moisture recharge in farmland

The different physical processes involved in soil water balance include rainfall or irrigation infiltration (Sun *et al.* 2018), soil water redistribution (Lopes *et al.* 2021), root water uptake (Hu *et al.* 2021), groundwater recharge (Yifru *et al.* 2021), and seepage from soil reservoirs (McCabe and Wolock 2020). In this study, the soil reservoirs were divided into shallow and deep soil moisture storage; the former referred to SMS in the 0–100 cm soil layer, and the latter identified as SMS in the 100–200 cm soil layer. Soil water balance in the shallow soil layers is affected by rainfall, runoff, irrigation, actual evapotranspiration, and soil water infiltrating into the deeper soil layer. The soil water balance in the deep soil layers is influenced by seepage from the upper soil layers and the deeper seepage that percolates out of the soil layer (Panigrahi and Panda 2003). Deep drainage is defined as the downward movement of soil water from the bottom of the root zone to the less active transmission zone, which is an essential component of water balance (McCabe and Wolock 2020). Deep drainage occurs in situations where SMC of the root zone is high, such as in the case of heavy precipitation and/or irrigation, which can recharge the groundwater aquifers (Liu *et al.* 2022). The data presents that the soil profiles experience dryness in June and early July annually due to

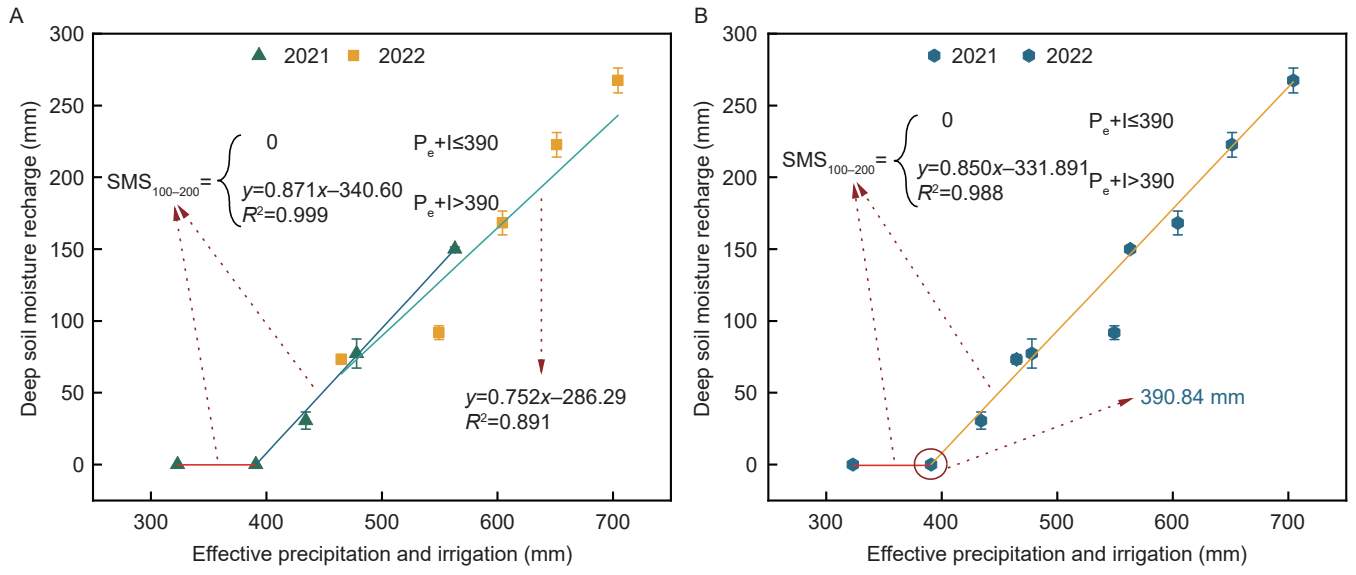


Fig. 7 Correlations between deep soil moisture recharge and effective precipitation and irrigation during summer maize growing seasons from 2021 to 2022 in Yangling, China. P_e, effective precipitation; I, irrigation amounts; $SMS_{100–200}$, deep soil moisture recharge in the 100–200 cm soil layer.

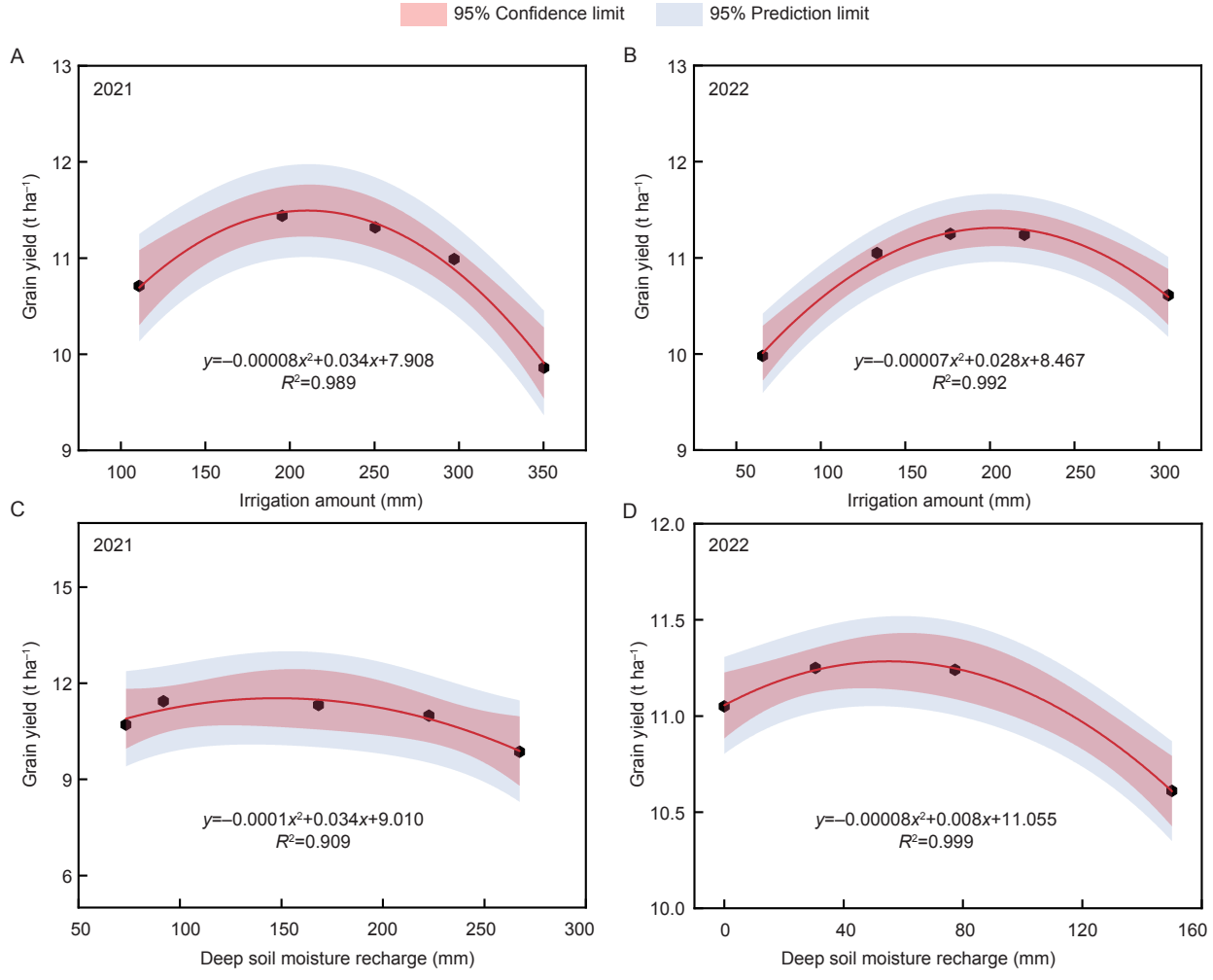


Fig. 8 Correlations between grain yield and irrigation amounts (A and B), and deep soil water recharge (C and D) during summer maize growing seasons from 2021 to 2022 in Yangling, China.

the limited rainfall and soil water consumption for summer maize, thereby resulting in the depletion of most of the water stored in the soil layers (Schomberg *et al.* 2023). The negative variations of $SMS_{0–100}$ was mainly caused by the combined effects of excessive evapotranspiration and low rainfall during the planting–V10 in 2021 (Fig. 6). The higher rainfall encourages plants development and compensates soil moisture loss induced by evapotranspiration, according to an earlier study (Wang *et al.* 2019). The precipitation distribution during planting–V10 in 2022 was more uniform than that in 2021, which alleviated water consumption in the shallow soil layers. The irrigation water increases available water amount for evapotranspiration, encourages soil moisture storage, and results in deep percolation and surface or lateral runoff (Jägermeyr *et al.* 2015). During the V10–VT period, the variations of $SMS_{0–100}$ and $SMS_{100–200}$ for different irrigation treatments significantly increased with an increase in irrigation amounts, and reached peak values under T5 treatment. Due to the higher concentrated irrigation (Table 1) and supplementary precipitation (Fig. 6) in 2021, the variations of $SMS_{0–100}$ was positive in 2021 and negative in 2022. A portion of the soil water flows out of the soil or percolates into deeper soil layers after rainfall stops, thereby recharging river networks or groundwater, which illustrates soil infiltration ability and rainfall regulation capacity (Yu *et al.* 2018). Moreover, a large amount of rainfall is more likely to recharge deep soil moisture through the root zone due to the shallow root zone of summer maize (Li *et al.* 2022). Thus, the heavy rainfall induced deep soil moisture storage during the R4–R6 in 2021. During the plant growth period, deep soil moisture was stable due to the heat insulation of the upper soil layer (Nakhforoosh *et al.* 2021). Although the irrigation upper limit and soil wetting layer depth was maintained consistently for the same irrigation treatment, the irrigation amounts showed significant differences between the two years. Specifically, the concentrated irrigation amounts in 2021 were significantly higher than those in 2022 under the same irrigation treatment. Thus, the deep soil moisture recharge induced by deep storage irrigation in 2021 was substantially higher than that in 2022. Overall, the total deep soil moisture recharge in 2021 attributed to heavy rainfall over the R4–R6 and higher concentrated irrigation amounts during V10–VT was significantly larger than in 2022.

In the double cropping system of summer maize and winter wheat, the irrigation management over one season impacts soil water balance for the other, particularly for crops cultivated in the rainy seasons (Lu Y *et al.* 2021). Winter wheat is supplied by soil water source accumulated during the maize growing seasons, particularly in the deep soil profile (Zhang *et al.* 2008). Therefore, deep soil moisture recharge over the summer maize seasons helps delay crop water shortage in the long absence of rainfall over the winter wheat seasons. Overall, the surface water can be fully used for irrigation in wet seasons, and even irrigation quotas can be appropriately increased to increase the deep soil moisture recharge, thereby reserving moisture sources for drought resistance, and the deep soil moisture storage can be utilized on site for irrigation applications in dry seasons (Dillon *et al.* 2019). These results are consistent with the theories previously demonstrated by Taylor *et al.* (2013) and Séraphin *et al.* (2016) that irrigation return flow is the fundamental source of groundwater recharge.

4.3. Effects of deep storage irrigation on maize grain yield

The relationships between GY and its responses to irrigation traits have been extensively documented (Ward 2022; Zhu *et al.* 2023; Zhang P A *et al.* 2024). The irrigation application is one of the most important elements influencing crop yields, and water is essential for improving crop productivity (Deb *et al.* 2022). It is conceivable for the volume of big pores, which are responsible for the drainage and aeration, to be reduced during irrigation stage (Drewry *et al.* 2021). The greater moisture availability are contributed to these processes under the conditions of enhanced irrigation amounts. Irrigation has been proven to increase maize yield (Chen *et al.* 2020). In this study, there was a quadratic curvilinear relationship between GY and irrigation amounts, which was also described by Payero *et al.* (2008), Irmak (2015a), and Irmak *et al.* (2020). Overall maize GY response to deep storage irrigation presented that the GY improved with applied irrigation increasing until T2 in 2021 and T3 in 2022, and then the curvilinear shape achieved the peak GY, which demonstrated that the excessive irrigation did not contribute to maize yield increase with further increase in irrigation amount and suggested diminishing returns (Irmak 2015b). Therefore, the appropriate irrigation increased accumulation and translocation of dry matter from tasseling to maturity stage, while the excessive irrigation resulted in a slight increase or even a decrease in maize yields. However, not much research has been reported on the practical threshold for excessive irrigation, and exceeding this threshold has no beneficial influences on the grain yield (Dixon 2015; Zhang *et al.* 2023). As previously noted, the T3 and T4 treatments showed decreases in GY of 1.0 and 3.9% in 2021, respectively, when compared to T2 treatment. In relative to T3 treatment, the GY for T5 treatment displayed a decrease of 5.7% in 2022. This is consistent with that excessive precipitation induced a loss of maize yields (Hu *et al.* 2023). These findings can be explained as short-term waterlogging induced by excessive irrigation decreased the available soil oxygen, reduced the aerobic microorganisms activity, and thereby gradually advanced the oxygen-depleted soil circumstances development (Wang *et al.* 2015). According to soil hypoxia and toxicity, the short-term waterlogging stress restricted maize yield formation whether directly by modifying roots metabolism or indirectly by limiting nutrient uptake (Bailey-Serres *et al.* 2012). Specifically, the adverse effects of short-term waterlogging stress on oxygen absorption in the root zone weakened the potential of the root system for nitrogen absorption and restricted nitrogen utilization efficiency, and ultimately resulted in a decline in the GY of maize (Zhang *et al.* 2023). Furthermore, the short-term waterlogging stress resulted in N loss, which hindered N uptake and transportation, and interrupted N cycle, and thus reduced GY of summer maize (Li *et al.* 2020; Yu *et al.* 2021). This may be the reason for the reduction in GY production

due to the further increase in irrigation amounts. Compared with the traditional deficit irrigation, plastic film mulching and no-till seeding and other measures, deep storage irrigation not only did not induce a reduction in maize yields, but showed the potential for yield improvement in some cases (Sithole and Magwaza 2019; Li and Wu 2022; Ning *et al.* 2024). Specifically, the maximum GY achieved under deep storage irrigation in this study (11.44 t ha^{-1}) was 4.95, 8.95, and 7.92% higher than the highest GY of the deficit irrigation (10.9 t ha^{-1}), ridge-furrow with plastic film mulching (10.5 t ha^{-1}), as well as no-till seeding (10.6 t ha^{-1}) reported by Ning *et al.* (2024), Li and Wu (2022), and Sithole and Magwaza (2019), respectively.

4.4. Limitations and recommendations

Despite this study has made some progress in deep storage irrigation, there are still several limitations that may potentially affect the accuracy and practical application value of the research results. Firstly, the definition of flood season is influenced by various factors, including climatic conditions, topography, and hydrological characteristics, which makes accurate and comprehensive determination quite challenging (Xu *et al.* 2023; Liu Y Z *et al.* 2024). This limitation may interfere with the determination of time for deep storage irrigation during the experimental process, and thereby affect the accuracy and reliability of these study results. The second limitation is nutrient leaching (i.e., N, P, and K) due to deep soil moisture recharge, and thereby decreases nutrient utilization efficiency and increases groundwater pollution risk, although deep drainage induced deep storage irrigation can recharge deep soil moisture and potentially recharge groundwater (Reading *et al.* 2019; Zhou and Zhao 2019). This limitation is particularly pronounced in coarse-textured soils, where the risks of nutrient leaching and subsequent groundwater contamination are higher owing to the combination of rapid water infiltration and diminished water retention capacity (Jílková and Angst 2022; Nepal *et al.* 2024). Thus, the applicability of these results may vary depending on the soil texture and structure. For example, the nutrient leaching losses are more significant in coarse-textured soils, while the enhanced water retention and nutrient immobilization can mitigate this risk in clay loam soil texture (Nano *et al.* 2016; Yuan *et al.* 2025). Therefore, the results of this study are applicable to clay loam soil texture and caution must be exercised when extrapolating these findings to coarser soils, finer soils, layered soils, or other agricultural soil environments characterized by distinct hydrological and nutrient dynamics. In addition, the further research should consider split nitrogen application to investigate the optimal proportion of base and topdressing applications of nitrogen fertilizer under deep storage irrigation conditions.

5. Conclusion

Results obtained in this study showed that the deep soil moisture recharge amounts and proportions to the sum of effective precipitation and irrigation significantly increased with irrigation amounts increasing, although induced only a slight decrease in grain yield. It can be concluded that this new technology of deep storage irrigation proposed in this study achieved deep soil moisture recharge, and ensured the maize grain yield was not significantly decreased. Overall, deep storage irrigation can recharge farmland deep soil moisture and sustain production of summer maize through flood resources utilization and can be popularized and applied in irrigation districts of northern China.

Acknowledgements

This work was supported by the National Natural Science Foundation of China (U2243235) and the Shaanxi Provincial Department of Water Resources, China (2022slkj-6).

Declaration of competing interest

The authors declare that they have no conflict of interest.

Declaration of generative AI and AI-assisted technologies in scientific writing process

The authors declare that they did not use AI in the preparation and writing of this manuscript.

References

Allen R G. 1998. *Crop Evapotranspiration-Guidelines for Computing Crop Water Requirements. Food and Agriculture Organization of the United Nations Irrigation and Drainage Paper*. Food and Agriculture Organization of the United Nations. p. 56.

Ayat H, Evans J P, Sherwood S C, Soderholm J. 2022. Intensification of subhourly heavy rainfall. *Science*, **378**, 655–659.

Bailey-Serres J, Lee S C, Brinton E. 2012. Water proofing crops: Effective flooding survival strategies. *Plant Physiology*, **160**, 1698–1709.

Camp M V, Radfar M, Walraevens K. 2010. Assessment of groundwater storage depletion by overexploitation using simple indicators in an irrigated closed aquifer basin in Iran. *Agricultural Water Management*, **97**, 1876–1886.

Cao Y X, Cai H J, Sun S K, Gu X B, Mu Q, Duan W N, Zhao Z X. 2022. Effects of drip irrigation methods on yield and water productivity of maize in Northwest China. *Agricultural Water Management*, **259**, 107227.

Chen S C, Wang S F, Shukla M K, Wu D, Guo X W, Li D H, Du T S. 2020. Delineation of management zones and optimization of irrigation scheduling to improve irrigation water productivity and revenue in a farmland of Northwest China. *Precision Agriculture*, **21**, 655–677.

Choi M, Jacobs J M. 2007. Soil moisture variability of root zone profiles within SMEX02 remote sensing footprints. *Advances in Water Resources*, **30**, 883–896.

Dastane N G. 1978. *Effective Rainfall in Irrigated Agriculture. Food and Agriculture Organization of the United Nations Irrigation and Drainage Paper*. Food and Agriculture Organization of the United Nations. p. 25.

Davenport F V, Burke M, Diffenbaugh N S. 2021. Contribution of historical precipitation change to US flood damages. *Proceedings of the National Academy of Sciences of the United States of America*, **118**, 1–7.

Deb P, Moradkhani H, Han X L, Abbaszadeh P, Xu L. 2022. Assessing irrigation mitigating drought impacts on crop yields with an integrated modeling framework. *Journal of Hydrology*, **609**, 127760.

Dillon P, Stuyfzand P, Grischek T, Lluria M, Pyne R D G, Jain R C, Bear J, Schwarz J, Wang W, Fernandez E, Stefan C, Pettenati M, van der Gun J, Sprenger C, Massmann G, Scanlon B R, Xanke J, Jokela P, Zheng Y, Rossetto R, *et al.* 2019. Sixty years of global progress in managed aquifer recharge. *Hydrogeology Journal*, **27**, 1–30.

Dixon G R. 2015. Water, irrigation and plant diseases. *CAB Reviews.: Perspectives in Agriculture, Veterinary Science, Nutrition and Natural Resources*, **10**, 10.

Drewry J J, Carrick S, Penny V, Houlbrooke D J, Laurenson S, Mesman N L. 2021. Effects of irrigation on soil physical properties

in predominantly pastoral farming systems: A review. *New Zealand Journal of Agricultural Research*, **64**, 483–507.
Famiglietti J S, Ryu D, Berg A A, Rodell M, Jackson T J. 2008. Field observations of soil moisture variability across scales. *Water Resources Research*, **44**, W01423.
Fan B Q, Zhang Y T, Fenton O, Daly K, Li J G, Wang H Y, Zhai L M, Luo X S, Lei Q L, Wu S X, Liu H B. 2024. Irrigation and nitrogen fertiliser optimisation in protected vegetable fields of northern China: Achieving environmental and agronomic sustainability. *Journal of Integrative Agriculture*, **23**, 1022–1033.
Fang H, Li Y N, Gu X B, Yu M, Du Y D, Chen P P, Li Y P. 2021. Evapotranspiration partitioning, water use efficiency, and maize yield under different film mulching and nitrogen application in northwest China. *Field Crops Research*, **264**, 108103.
Fu S J, Zhang H L, Zhong Q, Chen Q G, Liu A, Yang J, Pang J Z. 2023. Spatiotemporal variations of precipitation concentration influenced by large-scale climate factors and potential links to flood-drought events across China 1958–2019. *Atmospheric Research*, **282**, 106507.
Gao L, Shao M A. 2012. Temporal stability of soil water storage in diverse soil layers. *Catena*, **95**, 24–32.
Gao J, Xie P X, Zhuo L, Shang K H, Ji X X, Wu P T. 2021. Water footprints of irrigated crop production and meteorological driving factors at multiple temporal scales. *Agricultural Water Management*, **255**, 107014.
Gao Y, Zhou Z Q, Hao X M, Li T, Kang S Z. 2024. Spatio-temporal variability of soil water content across plot scales within a vineyard. *Journal of Hydrology*, **642**, 131882.
Guo Y P. 2009. On modern flood diersion and silt irrigation technology in Guanzhong area. MSc thesis, Shaanxi Normal University, China. (in Chinese)
Hershfield D M. 1964. Effective rainfall and irrigation water requirements. *Journal of Irrigation and Drainage Engineering*, **90**, 33–47.
Hidalgo H G, Alfaro E J, Quesada-Román A. 2024. Flood projections for selected Costa Rican main basins using CMIP6 climate models downscaled output in the HBV hydrological model for scenario SSP5-8.5. *Hydrological Research Letters*, **18**, 35–42.
Hu J, Yu W Z, Liu P, Zhao B, Zhang J W, Ren B Z. 2023. Responses of canopy functionality, crop growth and grain yield of summer maize to shading, waterlogging, and their combination stress at different crop stages. *European Journal of Agronomy*, **144**, 126761.
Hu J Y, Wu Y P, Wang L J, Sun P C, Zhao F B, Jin Z D, Wang Y Q, Qiu L J, Lian Y Q. 2021. Impacts of land-use conversions on the water cycle in a typical watershed in the southern Chinese Loess Plateau. *Journal of Hydrology*, **593**, 125741.
IPCC (Intergovernmental Panel on Climate Change). 2023. *Climate Change 2021-The Physical Science Basis: Working Group-Contribution to the Sixth Assessment Report of the Intergovernmental Panel on Climate Change*. Cambridge University Press, Cambridge, United Kingdom and New York, NY.
Irmak S. 2015a. Inter-annual variation in long-term center pivot-irrigated maize evapotranspiration (ET) and various water productivity response indices: Part I. Grain yield, actual and basal ET, irrigation-yield production functions, ET-yield production functions, and yield responses factors. *Journal of Irrigation and Drainage Engineering*, **141**, 1–17.
Irmak S. 2015b. Inter-annual variation in long-term center pivot-irrigated maize evapotranspiration (ET) and various water productivity response indices: Part II. Irrigation water use efficiency (IWUE1), crop WUE, evapotranspiration WUE, irrigation-evapotranspiration use efficiency, and precipitation use efficiency. *Journal of Irrigation and Drainage Engineering*, **141**, 1–11.
Irmak S, Mohammed A T, Kranz W L, Yonts C D, van Donk S. 2020. Irrigation-yield production functions and irrigation water use efficiency response of drought-tolerant maize hybrids under different irrigation levels, population densities and environments. *Sustainability*, **12**, 1–28.
Jägermeyr J, Gerten D, Heinke J, Schaphoff S, Kummu M, Lucht W. 2015. Water savings potentials of irrigation systems: Global simulation of processes and linkages. *Hydrology and Earth System Sciences*, **19**, 3073–3091.
James L. 1988. Principles of farm irrigation system design. CAB International, Wallingford, UK.
Ji Z M, Tian S T. 2024. A novel potential cause of extreme precipitation in the northwest China. *Heliyon*, **10**, e30826.
Jílková V, Angst G. 2022. Biochar and compost amendments to a coarse-textured temperate agricultural soil lead to nutrient leaching. *Applied Soil Ecology*, **173**, 104393.
Kanber R, Yazar A, Önder S, Köksal H. 1993. Irrigation response of pistachio (*Pistacia cera* L.). *Irrigation Science*, **14**, 1–14.
Kang S Z, Cai H J. 1996. *Agricultural Water Management*. China Agriculture Press, Beijing. (in Chinese)
Kendon E J, Fischer E M, Short C J. 2023. Variability conceals emerging trend in 100yr projections of UK local hourly rainfall extremes. *Nature Communications*, **14**, 1133.
Korres W, Reichenau T G, Fiener P, Koyama C N, Bogena H R, Cornelissen T, Baatz R, Herbst M, Diekkrüger B, Vereecken H, Schneider K. 2015. Spatio-temporal soil moisture patterns-A meta analysis using plot to catchment scale data. *Journal of Hydrology*, **520**, 326–341.
Li H, Si B C, Zhang Z Q, Miao C H. 2022. Deep soil water storage and drainage following conversion of deep rooted to shallow rooted vegetation. *Agricultural Water Management*, **261**, 107359.
Li Q, Du L J, Feng D J, Ren Y, Li Z X, Kong F L, Yuan J C. 2020. Grain-filling characteristics and yield differences of maize cultivars with contrasting nitrogen efficiencies. *The Crop Journal*, **8**, 990–1001.
Li X, Wu W. 2022. Can additional agricultural resource inputs improve maize yield, resource use efficiencies and emergy based system efficiency under ridge-furrow with plastic film mulching? *Journal of Cleaner Production*, **379**, 134711.
Liu C M, Zhang X Y, Zhang Y Q. 2002. Determination of daily evaporation and evapotranspiration of winter wheat and maize by large-scale weighing lysimeter and micro-lysimeter. *Agricultural and Forest Meteorology*, **111**, 109–120.
Liu H Y, Zou L, Xia J, Chen T, Wang F Y. 2022. Impact assessment of climate change and urbanization on the nonstationarity of extreme precipitation: A case study in an urban agglomeration in the middle reaches of the Yangtze river. *Sustainable Cities and Society*, **85**, 104038.
Liu Y Z, Wang C C, Jiang C B, Chin R J, Xiang Z H, Long Y N, Deng B, Wu Z Y. 2024. Water storage capacity estimation for a large complex lake system incorporating the water levels during flooding season. *Journal of Hydrology* (Regional Studies), **51**, 101634.
Liu Z J, Jiao L M, Lian X H. 2024. Impacts of increasing compound hot-dry events on vegetation under the warming-wetting trend in Northwest China. *Geography and Sustainability*, **6**, 100222.
Lopes T R, Zolin C A, Mingoti R, Vendrusculo L G, de Almeida F T, de Souza A P, de Oliveira R F, Paulino J, Uliana E M. 2021. Hydrological regime, water availability and land use/land cover change impact on the water balance in a large agriculture basin in the Southern Brazilian Amazon. *Journal of South American Earth Sciences*, **108**, 103224.
Lu J S, Geng C M, Cui X L, Li M Y, Chen S H, Hu T T. 2021. Response of drip fertigated wheat-maize rotation system on grain yield, water productivity and economic benefits using different water and nitrogen amounts. *Agricultural Water Management*, **258**, 107220.
Lu Y, Wang E L, Zhao Z G, Liu X W, Tian A L, Zhang X Y. 2021. Optimizing irrigation to reduce N leaching and maintain high crop productivity through the manipulation of soil water storage under summer monsoon climate. *Field Crops Research*, **265**, 108110.
Luo H X, Xu Y M, Han Q, Zhang L Q, Feng L. 2024. Remote sensing assessment of ecological quality of Baiyangdian wetland in response to extreme rainfall. *Remote Sensing Applications* (Society and Environment), **36**, 101284.
Mansouri-Far C, Sanavy S A M M, Saberali S F. 2010. Maize yield response to deficit irrigation during low-sensitive growth stages and nitrogen rate under semi-arid climatic conditions. *Agricultural Water Management*, **97**, 12–22.
McCabe G J, Wolock D M. 2020. The water-year water balance of the Colorado River basin. *Journal of the American Water Resources Association*, **56**, 724–737.
Morris B L, Lawrence A R L, Chilton P J C, Adams B, Calow R C, Klinck B A. 2003. Groundwater and its susceptibility to degradation: A global assessment of the problem and options for management. In: *Early Warning and Assessment Report Series*. United Nations Environment Programme, Nairobi, Kenya.
Nakhforoosh A, Nagel K A, Fiorani F, Bodner G. 2021. Deep soil exploration vs. topsoil exploitation: Distinctive rooting strategies between wheat landraces and wild relatives. *Plant and Soil*, **459**, 397–421.

Nano C C U, Nicolardot B, Quinche M, Munier-Jolain N, Ubertosi M. 2016. Effects of integrated weed management based cropping systems on the water retention of a silty clay loam soil. *Soil and Tillage Research*, **156**, 74–82.

Nepal J, Xin X P, Maltais-Landry G, Netto-Ferreira J B, Wright A, He Z L. 2024. Water dispersible carbon nanomaterials reduced N, P, and K leaching potential in sandy soils: A column leaching study. *Science of the Total Environment*, **954**, 176755.

Ning D F, Chen H Q, Qin A Z, Gao Y, Zhang J Y, Duan A W, Wang X P, Liu Z D. 2024. Optimizing irrigation and N fertigation regimes achieved high yield and water productivity and low N leaching in a maize field in the North China Plain. *Agricultural Water Management*, **301**, 108945.

Niu J, Zhu X G, Parry M A J, Kang S Z, Du T S, Tong L, Ding R S. 2019. Environmental burdens of groundwater extraction for irrigation over an inland river basin in Northwest China. *Journal of Cleaner Production*, **222**, 182–192.

Panigrahi B, Panda S N. 2003. Field test of a soil water balance simulation model. *Agricultural Water Management*, **58**, 223–240.

Payero J O, Tarkalson D D, Irmak S, Davison D, Petersen J L. 2008. Effect of irrigation amounts applied with subsurface drip irrigation on corn evapotranspiration, yield, water use efficiency, and dry matter production in a semiarid climate. *Agricultural Water Management*, **95**, 895–908.

Peng X B, Wang Y F, Ma J, Liu X A, Gu X B, Cai H J. 2023. Seasonal variation and controlling factors of carbon balance over dry semi-humid cropland in Guanzhong Plain. *European Journal of Agronomy*, **149**, 126912.

Pongpinyopap S, Mungcharoen T. 2012. Comparative study of green water footprint estimation methods for Thailand: A case study of cassava-based ethanol. *Environment and Natural Resources Journal*, **10**, 66–72.

Razaq M, Salahuddin, Shen H L, Sher H, Zhang P. 2017. Influence of biochar and nitrogen on fine root morphology, physiology, and chemistry of *Acer mono*. *Scientific Reports*, **7**, 5367.

Reading L, Bajracharya K, Wang J. 2019. Simulating deep drainage and nitrate leaching on a regional scale: Implications for groundwater management in an intensively irrigated area. *Irrigation Science*, **37**, 561–581.

Schomberg H H, White K E, Thompson A I, Bagley G A, Burke A, Garst G, Finley K A B, Mirsky S B. 2023. Interseeded cover crop mixtures influence soil water storage during the corn phase of corn-soybean-wheat no-till cropping systems. *Agricultural Water Management*, **278**, 108167.

Séraphin P, Vallet-Coulomb C, Gonçalvès J. 2016. Partitioning groundwater recharge between rainfall infiltration and irrigation return flow using stable isotopes: The Crau aquifer. *Journal of Hydrology*, **542**, 241–253.

Shan X Q, Cui N B, Cai H J, Hu X T, Zhao L. 2020. Estimation of summer maize evapotranspiration using MARS model in the semi-arid region of northwest China. *Computers and Electronics in Agriculture*, **174**, 105495.

Sithole N J, Magwaza L S. 2019. Long-term changes of soil chemical characteristics and maize yield in no-till conservation agriculture in a semi-arid environment of South Africa. *Soil and Tillage Research*, **194**, 104317.

Smith M. 1992. *CROPWAT a Computer Program for Irrigation Planning and Management*. *Food and Agriculture Organization of the United Nations Irrigation and Drainage Paper*. Food and Agriculture Organization of the United Nations, 46.

Su J X, Fan L X, Yuan Z L, Wang Z, Wang Z J. 2024. Quantifying the drought sensitivity of grassland under different climate zones in Northwest China. *Science of the Total Environment*, **910**, 168688.

Sun D, Yang H, Guan D X, Yang M, Wu J B, Yuan F H, Jin C J, Wang A Z, Zhang Y S. 2018. The effects of land use change on soil infiltration capacity in China: A meta-analysis. *Science of the Total Environment*, **626**, 1394–1401.

Sun H Y, Wang S F, Hao X M. 2017. An Improved Analytic Hierarchy Process Method for the evaluation of agricultural water management in irrigation districts of north China. *Agricultural Water Management*, **179**, 324–337.

Sun J, Niu W Q, Du Y D, Zhang Q, Li G C, Ma L, Zhu J J, Mu F, Sun D, Gan H C, Siddique K H M, Ali S. 2023. Combined tillage: A management strategy to improve rainfed maize tolerance to extreme events in northwestern China. *Agricultural Water Management*, **289**, 108503.

Tan L L, Zhang X L, Qi J Y, Sun D F, Marek G W, Feng P Y, Li B G, Liu D L, Li B G, Srinivasan R, Chen Y. 2023. Assessment of the sustainability of groundwater utilization and crop production under optimized irrigation strategies in the North China Plain under future climate change. *Science of the Total Environment*, **899**, 165619.

Taylor R G, Scanlon B, Döll P, Rodell M, van Beek R, Wada Y, Longuevergne L, Leblanc M, Famiglietti J S, Edmunds M, Konikow L, Green T R, Chen J Y, Taniguchi M, Bierkens M F P, MacDonald A, Fan Y, Maxwell R M, Yechieli Y, Gurdak J J, *et al.* 2013. Ground water and climate change. *Nature Climate Change*, **3**, 322–329.

Wang A F, Roitto M, Sutinen S, Lehto T, Heinonen J, Zhang G, Repo T. 2015. Waterlogging in late dormancy and the early growth phase affected root and leaf morphology in *Betula pendula* and *Betula pubescens* seedlings. *Tree Physiology*, **36**, 86–98.

Wang H, Xiang Y Z, Liao Z Q, Wang X, Zhang X Y, Huang X Y, Zhang F C, Feng L. 2024. Integrated assessment of water-nitrogen management for winter oilseed rape production in Northwest China. *Agricultural Water Management*, **298**, 108863.

Wang H, Zhang M T, Nan H W. 2019. Abiotic and biotic drivers of species diversity in understory layers of cold temperate coniferous forests in North China. *Journal of Forestry Research*, **30**, 2213–2225.

Wang H L, Wang Z Z, Zheng T L. 2018. Study on the present situation of groundwater resources and the networking of monitoring stations in Shannxi Province. *Ground Water*, **40**, 44–45, 49. (in Chinese)

Wang X L, Chen R S, Li H Y, Li K L, Liu J F, Liu G H. 2022. Detection and attribution of trends in flood frequency under climate change in the Qilian Mountains, Northwest China. *Journal of Hydrology* (Regional Studies), **42**, 101153.

Wang Z P, Zhang L, Wang B, Hou L Y, Xiao C W, Zhang X M, Han X G. 2018. Dissolved methane in groundwater of domestic wells and its potential emissions in arid and semi-arid regions of Inner Mongolia. China. *Science of the Total Environment*, **626**, 1193–1199.

Ward F A. 2022. Enhancing climate resilience of irrigated agriculture: A review. *Journal of Environmental Management*, **302**, 114032.

Wu F Q, Tang Q X, Cui J P, Tian L W, Guo R S, Wang L, Zheng Z P, Zhang N, Zhang Y J, Lin T. 2024. Deficit irrigation combined with a high planting density optimizes root and soil water-nitrogen distribution to enhance cotton productivity in arid regions. *Field Crops Research*, **317**, 109524.

Xu J, Li X F, Wan W L, Zhu X L, Li C H, Zhao X W, Zhao Y H, Pang S Q, Diao M. 2024. Impact of regulated deficit irrigation on the dynamics of quality changes in processing tomato fruits during ripening. *Agricultural Water Management*, **304**, 109068.

Xu Z X, Mo L, Zhou J Z, Zhang X. 2023. Optimal dispatching rules of hydropower reservoir in flood season considering flood resources utilization: A case study of Three Gorges Reservoir in China. *Journal of Cleaner Production*, **388**, 135975.

Yan S C, Wu Y, Fan J L, Zhang F C, Zheng J, Guo J J, Lu J S, Wu L F, Qiang S C, Xiang Y Z. 2022. Source-sink relationship and yield stability of two maize cultivars in response to water and fertilizer inputs in northwest China. *Agricultural Water Management*, **262**, 107332.

Yan Z J, Zhou J, Yang L, Gunina A, Yang Y D, Peixoto L, Zeng Z H, Zang H D, Kuzyakov Y. 2022. Diversified cropping systems benefit soil carbon and nitrogen stocks by increasing aggregate stability: Results of three fractionation methods. *Science of the Total Environment*, **824**, 153878.

Yang B, Yue S C, Gao N, Wei Y N, Shen Y F, Zhan A, Li S Q. 2023. Effects of the key environmental and management factors on the advantages of film mulching spring maize in northwest China: A meta-analysis. *European Journal of Agronomy*, **150**, 126947.

Yang J, Li G Q, Gan Y X, Chen Z F, Zhang X J. 2023. Role of the tropical Indian Ocean in orbitally induced mid-Holocene precipitation variation in northwest China. *Quaternary Science Reviews*, **317**, 108285.

Yang W J, Li Y L, Liu W J, Wang S W, Yin L N, Deng X P. 2021. Sustainable high yields can be achieved in drylands on the Loess Plateau by changing water use patterns through integrated agronomic management. *Agricultural and Forest Meteorology*, **296**, 108210.

Yifru B A, Chung I M, Kim M G, Chang S W. 2021. Assessing the effect of land/use land cover and climate change on water yield and groundwater recharge in East African Rift Valley using integrated

model. *Journal of Hydrology* (Regional Studies), **37**, 100926.
Yin J B, Guo S L, Gentine P, Sullivan S C, Gu L, He S K, Chen J, Liu P. 2021. Does the hook structure constrain future flood intensification under anthropogenic climate warming? *Water Resources Research*, **57**, WR028491.
Yost J L, Huang J Y, Hartemink A E. 2019. Spatial-temporal analysis of soil water storage and deep drainage under irrigated potatoes in the Central Sands of Wisconsin, USA. *Agricultural Water Management*, **217**, 226–235.
Yu B Q, Xie C K, Cai S Z, Chen Y, Lv Y P, Mo Z L, Liu T L, Yang Z W. 2018. Effects of tree root density on soil total porosity and non-capillary porosity using a ground-penetrating tree radar unit in Shanghai, China. *Sustainability*, **10**, 4640.
Yu Y M, Xu J Z, Zhang P C, Meng Y, Xiong Y J. 2021. Controlled irrigation and drainage reduce rainfall runoff and nitrogen loss in paddy fields. *International Journal of Environmental Research and Public Health*, **18**, 3348.
Yuan H W, Cui Y, Jiang S M, Tang G M, Yuan X J. 2018. Estimation of maize evapotranspiration under drought stress based on large-scale lysimeter and genetic algorithm. *Transactions of the Chinese Society for Agricultural Machinery*, **49**, 333–342.
Yuan T A, Tai A P K, Mao J, Li R K K, Wu J, Li S. 2023. Effects of different irrigation methods on regional climate in North China Plain: A modeling study. *Agricultural and Forest Meteorology*, **342**, 109728.
Yuan X M, Ban G C, Luo Y B, Wang J R, Peng D J, Liang R, He T G, Wang Z T. 2025. Biochar effects on aggregation and carbon-nitrogen retention in different-sized aggregates of clay and loam soils: A meta-analysis. *Soil and Tillage Research*, **247**, 106365.
Zagaria C, Schulp C J E, Zavalloni M, Viaggi D, Verburg P H. 2021. Modelling transformational adaptation to climate change among crop farming systems in Romagna, Italy. *Agricultural Systems*, **188**, 103024.
Zhang C, Xie Z A, Wang Q J, Tang M, Feng S Y, Cai H J. 2022. AquaCrop modeling to explore optimal irrigation of winter wheat for improving grain yield and water productivity. *Agricultural Water Management*, **266**, 107580.
Zhang H W, Liang Q, Peng Z P, Zhao Y, Tan Y C, Zhang X, Bol R. 2023. Response of greenhouse gases emissions and yields to irrigation and straw practices in wheat-maize cropping system. *Agricultural Water Management*, **282**, 108281.
Zhang P A, Li M, Fu Q, Singh V P, Du C Z, Liu D, Li T X, Yang A Z. 2024. Dynamic regulation of the irrigation-nitrogen-biochar nexus for the synergy of yield, quality, carbon emission and resource use efficiency in tomato. *Journal of Integrative Agriculture*, **23**, 680–697.
Zhang P Y, Liu J Z, Wang M D, Zhang H C, Yang N, Ma J, Cai H J. 2024. Effects of irrigation and fertilization with biochar on the growth, yield, and water/nitrogen use of maize on the Guanzhong Plain, China. *Agricultural Water Management*, **295**, 108786.
Zhang Q S, Sun J H, Dai C L, Zhang G X, Wu Y F. 2024. Sustainable development of groundwater resources under the large scale conversion of dry land into rice fields. *Agricultural Water Management*, **298**, 108851.
Zhang X Y, Chen S Y, Sun H Y, Pei D, Wang Y M. 2008. Dry matter, harvest index, grain yield and water use efficiency as affected by water supply in winter wheat. *Irrigation Science*, **27**, 1–10.
Zhao H B, Liu G F, Dou Y X, Yang H M, Wang T, Wang Z H, Malhi S, Khan A A. 2024. Plastic mulch increases dryland wheat yield and water-use productivity, while straw mulch increases soil water storage. *Journal of Integrative Agriculture*, **23**, 3174–3185.
Zhao K A, Wang H T, Wu J Z, Liu A, Huang X L, Li G Q, Wu S W, Zhang J, Zhang Z W, Hou Y Q, Zhao Z M, Li S, Guo J H, Zhao W X, Li S J, Li W N, Huang M, Li Y J. 2023. One-off irrigation improves water and nitrogen use efficiency and productivity of wheat as mediated by nitrogen rate and tillage in drought-prone areas. *Field Crops Research*, **295**, 108898.
Zhou H, Zhao W Z. 2019. Modeling soil water balance and irrigation strategies in a flood-irrigated wheat-maize rotation system. A case in dry climate, China. *Agricultural Water Management*, **221**, 286–302.
Zhou S L, Wu Y C, Wang Z M, Lu L Q, Wang R Z. 2008. The nitrate leached below maize root zone is available for deep-rooted wheat in winter wheat-summer maize rotation in the North China Plain. *Environmental Pollution*, **152**, 723–730.
Zhu R M, Zhao R Q, Li X J, Hu X Y, Jiao S X, Xiao L A, Xie Z X, Sun J, Wang S, Yang Q L, Zhang H F, Chuai X W. 2023. The impact of irrigation modes on agricultural water-energy-carbon nexus. *Science of the Total Environment*, **860**, 160493.

Executive Editor-in-Chief Jinshui Wu
Managing Editor Lujuan Sun